



Det här verket är upphovrättskyddat enligt *Lagen (1960:729) om upphovsrätt till litterära och konstnärliga verk*. Det har digitaliserats med stöd av Kap. 1, 16 § första stycket p 1, för forskningsändamål, och får inte spridas vidare till allmänheten utan upphovsrättsinnehavarens medgivande.

Alla tryckta texter är OCR-tolkade till maskinläsbar text. Det betyder att du kan söka och kopiera texten från dokumentet. Vissa äldre dokument med dåligt tryck kan vara svåra att OCR-tolka korrekt vilket medför att den OCR-tolkade texten kan innehålla fel och därför bör man visuellt jämföra med verkets bilder för att avgöra vad som är riktigt.

This work is protected by Swedish Copyright Law (*Lagen (1960:729) om upphovsrätt till litterära och konstnärliga verk*). It has been digitized with support of Kap. 1, 16 § första stycket p 1, for scientific purpose, and may no be disseminated to the public without consent of the copyright holder.

All printed texts have been OCR-processed and converted to machine readable text. This means that you can search and copy text from the document. Some early printed books are hard to OCR-process correctly and the text may contain errors, so one should always visually compare it with the images to determine what is correct.



**Designed folded polypeptide model systems for the
study of enzyme mimicking reactions**

Martin Kjellstrand



**Department of Chemistry
Organic Chemistry, Göteborg University
Göteborg, Sweden
1998**



Biomedicinska biblioteket

Din

98.401

Designed folded polypeptide model systems for the study of enzyme mimicking reactions

Martin Kjellstrand



Akademisk avhandling för avläggande av filosofie doktorsexamen i kemi som enligt beslut av tjänsteförslagsnämndens ordförande kommer att försvaras offentligt tisdagen den 2 juni 1998 kl 10.15 i föreläsningssal KA, Kemigården 5, Göteborgs universitet och Chalmers Tekniska Högskola. Avhandlingen kommer att försvaras på engelska.

Fakultetsopponent är Dr. Adrian George, School of Chemistry, University of Sydney, Sydney, Australia.

Department of Chemistry

Göteborg University

1998

Martin Kjellstrand, **Designed folded polypeptide model systems for the study of enzyme mimicking reactions**, 1998. Department of Chemistry, Organic Chemistry, Göteborg University, Göteborg, Sweden. ISBN 91-628-3035-X

ABSTRACT

Designed folded polypeptides have been used as templates for model systems for the study of three different enzyme mimicking reactions.

A NAD⁺ analogue has been synthesised and incorporated into a folded polypeptide with a helix-loop-helix motif by a site-selective self-functionalisation reaction. The success of the incorporation reaction was shown by ESMS and two-dimensional NMR spectroscopy. The solution structure of the polypeptide was not affected by the incorporation of the cofactor model as shown by NMR and CD spectroscopy. The peptide-bound NAD⁺ analogue was reduced faster and its lifetime was increased by more than a factor of three compared to that of 1-methylnicotinamide. The modified peptide is water soluble which is a requirement for the creation of a turnover system.

PP-42, a 42-residue folded polypeptide, has been designed to form an aldimine with pyridoxal phosphate (PLP). The site-selectivity was shown to be controlled by non-covalent interactions between the cofactor and a single arginine residue in the reactive site. PP-42 has been synthesised and shown to incorporate PLP covalently as an aldimine by UV spectroscopy and LC-ESMS. The incorporation of the cofactor did not affect the solution structure of PP-42 adversely. The site-selectivity of the incorporation has been determined by trypsin digestion of the reduced functionalised peptide. In a control experiment where pyridoxal hydrochloride was used instead of PLP no significant amount of aldimine formation was observed.

NP-42, a 42-residue polypeptide, has been designed to catalyse the decarboxylation of oxaloacetate. The reaction rate of the peptide catalysed decarboxylation of oxaloacetate has been measured by UV and NMR spectroscopy. NP-42 is found to catalyse the decarboxylation of oxaloacetate with a second order rate constant of $0.01 \text{ M}^{-1} \text{ s}^{-1}$. A comparison has been made between the second-order rate constants obtained by the different spectroscopic techniques. ¹H NMR spectroscopy allows the direct observation of both reactant and product simultaneously.

Keywords: NAD⁺, NADH, enzyme mimic, folded polypeptides, transamination, pyridoxal phosphate, oxaloacetate, decarboxylation, design, site-selective, self-functionalisation, incorporation, non-covalent control.

Designed folded polypeptide model systems for the study of enzyme mimicking reactions

Martin Kjellstrand



Department of Chemistry
Organic Chemistry, Göteborg University
Göteborg, Sweden

1998

"Understanding is a three-edged sword."

Kosh Naranek of *Babylon 5*

© Martin Kjellstrand 1998.

ISBN 91-628-3035-X

ABSTRACT

Designed folded polypeptides have been used as templates for model systems for the study of three different enzyme mimicking reactions.

A NAD⁺ analogue has been synthesised and incorporated into a folded polypeptide with a helix-loop-helix motif by a site-selective self-functionalisation reaction. The success of the incorporation reaction was shown by ESMS and two-dimensional NMR spectroscopy. The solution structure of the polypeptide was not affected by the incorporation of the cofactor model as shown by NMR and CD spectroscopy. The peptide-bound NAD⁺ analogue was reduced faster and its lifetime was increased by more than a factor of three compared to that of 1-methylnicotinamide. The modified peptide is water soluble which is a requirement for the creation of a turnover system.

PP-42, a 42-residue folded polypeptide, has been designed to form an aldimine with pyridoxal phosphate (PLP). The site-selectivity was shown to be controlled by non-covalent interactions between the cofactor and residues in the reactive site. PP-42 has been synthesised and shown to incorporate PLP covalently as an aldimine by UV spectroscopy and LC-ESMS. The incorporation of the cofactor did not affect the solution structure of PP-42 adversely. The site-selectivity of the incorporation has been determined by trypsin digestion of the reduced functionalised peptide. In a control experiment where pyridoxal hydrochloride was used instead of PLP no significant amount of aldimine formation was observed.

NP-42, a 42-residue polypeptide, has been designed to catalyse the decarboxylation of oxaloacetate. The reaction rate of the peptide catalysed decarboxylation of oxaloacetate has been measured by UV and NMR spectroscopy. NP-42 is found to catalyse the decarboxylation of oxaloacetate with a second order rate constant of $0.01 \text{ M}^{-1} \text{ s}^{-1}$. A comparison is made between the second-order rate constants obtained from the different spectroscopic techniques as well as with those of catalysts reported in the literature. ¹H NMR spectroscopy allows the direct observation of both reactant and product simultaneously.

Keywords: NAD⁺, NADH, enzyme mimic, folded polypeptides, transamination, pyridoxal phosphate, oxaloacetate, decarboxylation, design, site-selective, self-functionalisation, incorporation, non-covalent control.

List of publications

This thesis is based partly on the following papers:

I. The site-selective incorporation of a NAD⁺ cofactor mimic into a folded helix-loop-helix motif.

Martin Kjellstrand, Klas Broo, Linda Andersson, Åke Nilsson, and Lars Baltzer.

J. Chem. Soc., Perkin Trans. 2, **1997**, 2745.

II. Non-covalent control of site-selective incorporation of the pyridoxal phosphate cofactor into a folded polypeptide motif - mimicking a key step in enzymatic transamination.

Malin Allert, Martin Kjellstrand, Klas Broo, Åke Nilsson, and Lars Baltzer.

J. Chem. Soc., Chem. Commun., Accepted for publication.

III. A designed folded polypeptide model system that catalyses the decarboxylation of oxalacetate.

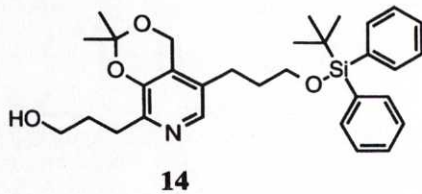
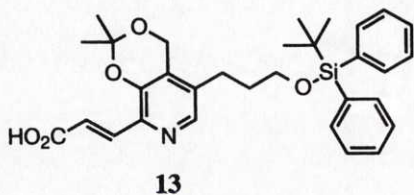
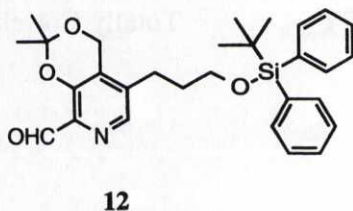
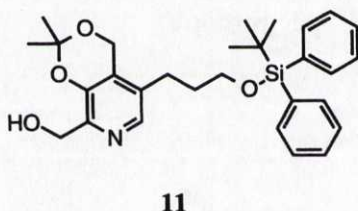
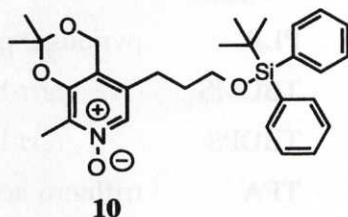
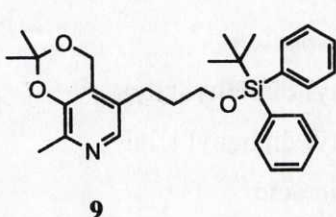
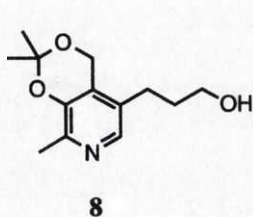
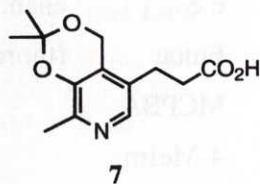
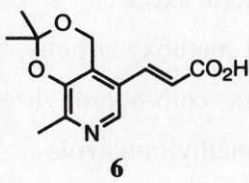
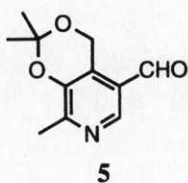
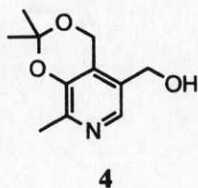
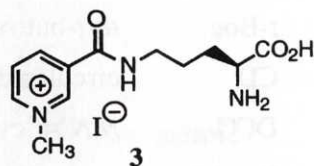
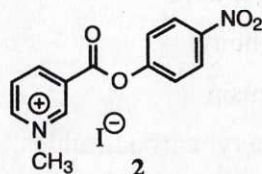
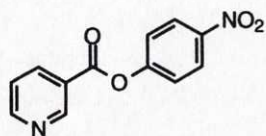
Martin Kjellstrand, Malin Allert, Klas Broo, Åke Nilsson, and Lars Baltzer.

J. Chem., Soc., Perkin Trans. 2, submitted for publication.

List of abbreviations

Aib	amino isobutyric acid
<i>t</i> -Boc	<i>tert</i> -butoxycarbonyl
CD	circular dichroism
DCC	<i>N,N'</i> -dicyclohexyl carbodiimide
DMAP	<i>N,N</i> -dimethylamino pyridine
e.e.	enantiomeric excess
Fmoc	fluorenyl methoxycarbonyl
MCPBA	<i>meta</i> -chloroperoxybenzoic acid
4-MeIm	4-methylimidazole
NAD	nicotinamide adenine dinucleotide
NOESY	Nuclear Overhauser Effect Spectroscopy
PLP	pyridoxal phosphate
TBDMS	<i>tert</i> -butyl dimethyl silyl
TBDPS	<i>tert</i> -butyl diphenyl silyl
TFA	trifluoro acetic acid
TFAA	trifluoro acetic anhydride
TOCSY	Totally Correlated Spectroscopy

Molecular structures of the nonpeptide compounds investigated



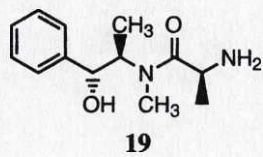
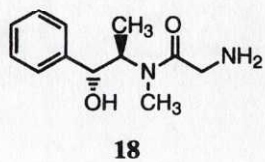
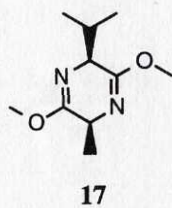
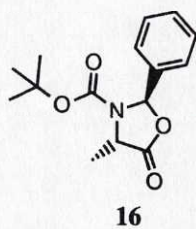
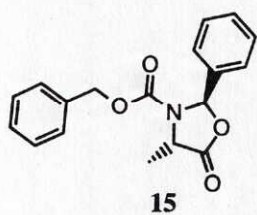


Table of contents

1. Introduction	1
2. Enzyme reactions studied in model systems	3
2.1 The NAD ⁺ /NADH cofactor and model systems	3
2.2 The pyridoxal phosphate cofactor and model systems	6
2.3 Artificial decarboxylases	12
2.4 Summary	15
3. Polypeptide design, structure, and reactivity	16
3.1 Rational design of polypeptides	16
3.2 Design and structure of SA-42 and RA-42	16
3.3 The reactivity of RA-42	18
3.4 The site-selectivity of RA-42	18
4. Folded polypeptide model systems	20
5. The preparation of a NAD ⁺ /NADH model system by post-synthetic modification of a folded polypeptide: RA-42NAD and LA-42NAD	21
5.1 The structure of RA-42	21
5.2 Synthesis of the NAD ⁺ cofactor mimics	22
5.3 Incorporation of the NAD ⁺ cofactor mimic into RA-42 and LA-42	23
5.4 The structure of LA-42NAD	24
5.5 Reduction of LA-42NAD into LA-42NADH	25
5.6 Reduction of α,α,α -trifluoro acetophenone using LA-42NADH	27
5.7 Summary	28
6. Non-covalent control of site-selective incorporation: PP-42 and pyridoxal phosphate	29
6.1 The design of PP-42	29
6.2 The structure of PP-42	31
6.3 Incorporation of pyridoxal phosphate into PP-42	31
6.4 An attempted transamination between glutamic acid and pyridoxal phosphate	36
6.5 Summary	37
7. Catalysis of the decarboxylation of oxaloacetate: NP-42	39
7.1 The design of NP-42	39
7.2 The structure of NP-42	40
7.3 Study of the NP-42 catalysed decarboxylation of oxaloacetate	41
7.4 The reactivity of NP-42	45
7.5 Summary	46

8. Preparation of a cyclic hexapeptide model system for the study of transamination reactions.....	48
8.1 Cyclic hexapeptides.....	48
8.2 Design of the cyclic hexapeptide model system.....	48
8.3 Design and synthesis of a two-armed pyridoxine derivative for incorporation into a cyclic hexapeptide.....	49
8.4 Asymmetric α -amino acid synthesis.....	51
8.4.1 The Mutter approach to α -methylated α -amino acids.....	51
8.4.2 The Schoellkopf <i>bis</i> -lactim ether method.....	52
8.4.3 The pseudoephedrine method of Myers.....	53
8.5 Summary.....	53
9. Summary and outlook.....	55
10. Methods.....	57
10.1 Peptide synthesis.....	57
10.2 HPLC.....	59
10.3 NMR spectroscopy.....	59
10.4 CD spectroscopy.....	60
10.5 Electrospray mass spectrometry.....	60
11. Experimental.....	61
11.1 General.....	61
11.2 Peptide synthesis and purification.....	62
11.3 Synthesis of the nonpeptide structures.....	63
11.3.1 NAD ⁺ analogues and model systems.....	63
11.3.2 Syntheses of the cyclohexapeptide project.....	65
11.4 Cofactor model incorporations.....	71
11.5 Kinetics and reaction studies.....	71
12. Acknowledgements.....	75

1. Introduction

The study of enzymatic reactions through model systems¹ enhances our understanding of the mechanisms behind their catalytic efficiency. Such knowledge satisfies the curiosity of chemists but it can also most importantly be applied in the design and engineering of new catalysts with novel functions. The efficiency and reactivity of biocatalysts is due to interplay between a large number of groups in complex three-dimensional structures.

The secondary and tertiary structures of an enzyme is dependent on its amino acid sequence, and the active site of an enzyme is often located in a hydrophobic crevice. It contains a large number of functional groups for substrate and cofactor binding, and for catalysis. The goal in the study of model systems is to clarify the role of each interaction.

Key features of enzymes targeted in enzyme mimickry include achieving reaction rate enhancements, substrate recognition, turnover, and stereospecific catalysis. An enzyme mimic with the properties of a native enzyme has not yet been achieved. Key problems include those of synthesis, solubility, and catalyst rigidity.

Folded polypeptides have so far not been used to any large extent in enzyme mimicking in spite of the facts that they are likely to ensure the solubilities of model systems in aqueous solutions and that they are large enough to allow the incorporation of groups capable of substrate recognition and transition state binding. The reactive site of folded

¹ a) Murakami, Y.; Kikuchi, J.-I.; Hisaeda, Y.; Hayashida, O. *Chem. Rev.* **1996**, *96*, 721.

b) Menger, F. M. *Acc. Chem. Res.* **1993**, *26*, 206.

c) Kirby, A. J. *Angew. Chem. Int. Ed. Engl.* **1996**, *35*, 707.

polypeptides may also be systematically varied by minor modifications of the amino acid sequence that leaves the tertiary structure unchanged.

This thesis presents some of the first examples of folded polypeptide model systems for enzyme mimicking reactions. Three different strategies have been used in the design. A one-step site-selective self-functionalisation reaction has been used to incorporate a NAD⁺ cofactor model into a folded polypeptide motif. The pyridoxal phosphate cofactor has been incorporated into a four-helix bundle with the site-selectivity of the incorporation controlled by non-covalent interactions. Finally, a reactive site has been designed for the catalysis of the decarboxylation of oxaloacetate where only the naturally occurring amino acids have been used.

2. Enzyme reactions studied in model systems

2.1 The $NAD^+/NADH$ cofactor and model systems

The dehydrogenase class of enzymes perform redox reactions in metabolic systems² by utilising the $NAD^+/NADH$ cofactor for hydride-transfer reactions, Figure 1.

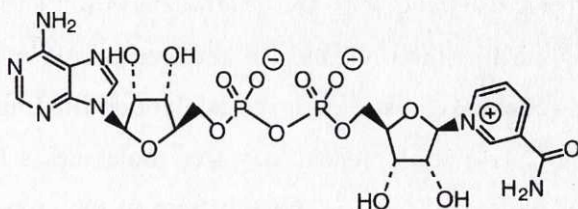


Figure 1. Nicotinamide adenine dinucleotide, NAD^+ .

The residue responsible for the catalytic activity is the nicotinamide moiety, which exists in two redox forms, Figure 2.

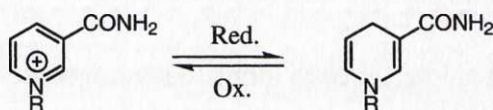


Figure 2. The $NAD^+/NADH$ redox couple.

The reduced cofactor ($NADH$) can deliver one of the hydrogens in 4-position of the nicotinamide residue as a hydride ion to a carbonyl group and reduce it to the corresponding alcohol. In the reverse reaction, a hydride ion is abstracted from the substrate in an oxidation reaction. The hydrogens at position 4 are prochiral³, Figure 3. The transfer of a hydride ion from $NADH$ to a substrate

² Dugas, H. *Bioorganic Chemistry*, 3rd edition, 1996, Springer-Verlag, New York.

³ Fersht, A. *Enzyme Structure and Mechanism*, 2nd edition, 1985, 226, W. H. Freeman, New York.

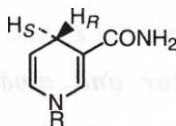


Figure 3. The prochiral 4-hydrogens of NADH.

is direct and stereospecific⁴. The alcohol dehydrogenases are metalloenzymes that use zinc ions for their catalysis⁵. The Zn²⁺-ion is bound by serine and histidine residues at the bottom of a hydrophobic pocket that joins the catalytic site with the nucleotide-binding part of the enzyme. When no substrate is present, a water molecule is bound to the zinc ion. This water is displaced by the substrate in the enzyme-substrate complex. Lactate dehydrogenase (LDH), lacks a zinc ion in the active site and its role is taken over by a histidine and an arginine⁶. A second arginine residue is positioned to stabilise the transition state during the hydride transfer reaction. The stereospecific transfer of the hydride ion is the basis for the stereospecificity of the dehydrogenases.

Model systems that are designed to mimic dehydrogenase activity must be able to incorporate some of the control mechanisms used by the dehydrogenases for stereospecificity. To achieve this in enzyme mimics, a way of imposing the required three-dimensional restrictions upon the hydride transfer must be found.

The NAD⁺/NADH system has been modelled extensively⁷. Studies of NAD⁺ models for mechanistic purposes have been pursued since 1951,

⁴ Fisher, H. F.; Conn, E. E.; Vennesland, B.; Westheimer, F. H. *J. Biol. Chem.* **1953**, *202*, 687.

⁵ Brändén, C.-I.; Jornvall, H.; Eklund, H.; Furugren, B. *The Enzymes* **1975**, *11*, 104.

⁶ Parker, D. M.; Holbrook, J. J. *Pyridine Nucleotide Dependent Dehydrogenases*, **1977**, Sund, H. (ed), Walter de Gruyter, Berlin, p 485.

⁷ Yasui, S.; Ohno, A. *Bioorg. Chem.* **1986**, *70*.

when Westheimer⁸ and co-workers studied the mechanism of hydride transfer by using deuterium as a tracer in the investigation of the mechanism of NAD⁺-mediated ethyl alcohol oxidation to acetaldehyde.

In the reduction of ethyl benzoylformate in acetonitrile by the reduced form of 1-benzylnicotinamide (BNAH), Ohno and co-workers have shown that the reaction does not proceed unless an equimolar amount of Mg²⁺-ion is present⁹, and that the reaction rate of the reduction of trifluoroacetophenone (TFAB) is dependent on the concentration of Mg²⁺-ion¹⁰.

When the reaction medium was changed from DMSO to water in the reduction of TFAB by 1-*n*-propylnicotinamide (PNAH), a reaction rate enhancement by a factor of 5000 was achieved by van Eikeren *et al*¹¹.

In order to attack the problem of stereoselectivity in the reaction, Meyers attached a glyoxylic acid residue to a modified cofactor analogue, Figure 4, and made the Zn²⁺-mediated reaction intramolecular¹².

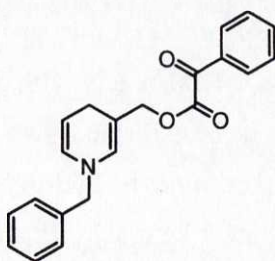


Figure 4. The intramolecular NADH model used by Meyers.

⁸ Westheimer, F. H.; Fisher, H. F.; Conn, E. E.; Vennesland, B. *J. Am. Chem. Soc.* **1951**, *73*, 2463.

⁹ Onishi, Y.; Kagami, M.; Ohno, A. *J. Am. Chem. Soc.* **1975**, *97*, 4766.

¹⁰ Ohno, A.; Yamamoto, H.; Oka, S. *J. Am. Chem. Soc.* **1981**, *103*, 2041.

¹¹ van Eikeren, P.; Grier, D. L. *J. Am. Chem. Soc.* **1976**, *98*, 4655.

¹² Meyers, A. I.; Brown, J. D. *J. Am. Chem. Soc.* **1987**, *109*, 3155.

The intramolecularity had the added advantage of not only inducing stereoselectivity, but also of enhancing the reaction rate significantly.

NADH model systems bound to a cyclodextrine unit, synthesised by Toda and co-workers¹³, were used to investigate substrate binding as a means for reaction rate enhancement. These model systems gave rate enhancements by a factor of 50 in the reduction of ninhydrin in comparison with that of the reduction by NADH.

These model systems have all attempted to mimic some aspects of the dehydrogenases. Partial solutions to the problems of stereoselectivity, metal ion coordination, and rate enhancements have been proposed. The problem of achieving a turnover system has so far not been solved, probably because most NAD⁺/NADH mimics are insoluble in water. The most efficient way of regenerating the reduced form of the catalyst, by sodium dithionite, requires water as solvent.

2.2 The pyridoxal phosphate cofactor and model systems

The cofactor pyridoxal phosphate (PLP) is an important factor in the metabolism of α -amino acids¹⁴. PLP reacts with an amino acid to form a Schiff base aldimine, which is transformed into a ketimine through an allylic rearrangement. The ketimine is hydrolysed by water, to form pyridoxamine phosphate and an α -keto acid, Figure 5.

¹³ Yoon, C.-J.; Ikeda, H.; Kojin, R.; Ikeda, T.; Toda, F. *J. Chem. Soc., Chem. Commun.* **1986**, 1080.

¹⁴ a) Snell, E. E.; di Mari, S. J. *The Enzymes* **1976**, 2, 335.

b) Davis, L.; Metzler, D. E. *The Enzymes* **1972**, 7, 33.

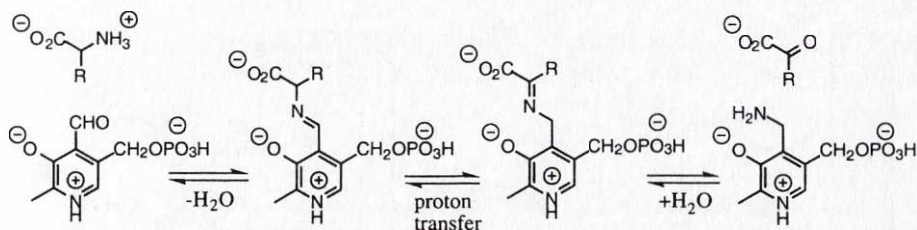


Figure 5. The reaction sequence of the pyridoxal- or pyridoxamine-mediated transamination.

The reaction is performed by a class of enzymes known as aminotransferases that are essential for the biosynthesis of α -amino acids. The exception is L-glutamic acid, for which the nitrogen is provided by ammonia, through an NADH-mediated reductive amination of 2-oxoglutarate. In the aminotransferase catalysed reactions a proton from the solvent is incorporated at the α -carbon of the formed amino acid¹⁵, and the β hydrogen of that amino acid does not participate in the reaction¹⁶. The pyridoxal is initially bound covalently as an aldimine Schiff base to the enzyme¹⁷, and is then displaced by the substrate amino acid, under the formation of a new Schiff base as shown in figure 6.

¹⁵ Hilton, M. A.; Barnes, Jr., F. W.; Enns, T. *J. Biol. Chem.* **1956**, *219*, 83.

¹⁶ a) Meister, A. *Nature* **1957**, *168*, 1119.

b) Sprinson, D. B.; Rittenberg, D. *J. Biol. Chem.* **1950**, *184*, 405.

c) Gisolia, S. B.; Burris, R. H. *J. Biol. Chem.* **1954**, *210*, 109.

¹⁷ Hughes, R. C.; Jenkins, W. T.; Fischer, E. H. *Proc. Natl. Acad. Sci. USA*, **1962**, *48*, 1615.

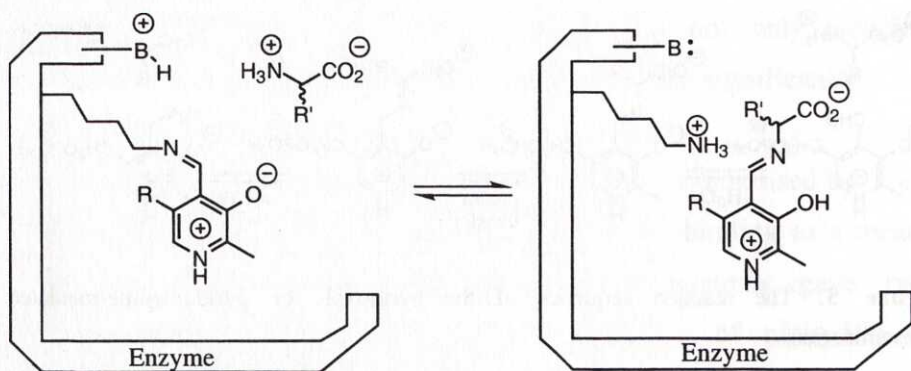


Figure 6. The binding of the substrate amino acid to the enzyme-bound pyridoxal. R = $\text{CH}_2\text{OPO}_3\text{H}^-$, R' = amino acid side chain.

The Schiff base formation and subsequent rearrangements are promoted by the pyridinium ion that functions as an electron sink. The reaction has been thoroughly investigated in aspartate aminotransferase¹⁸. The pyridoxal-bound substrate is stabilised through the interactions with two arginine residues, Arg-292 and Arg-386. The phenolic group is hydrogen-bonded to the hydroxyl of Tyr-225 while the pyridine ring nitrogen is hydrogen-bonded to Asp-222. The 5'-phosphate group is bound by several amino acid residues, including Arg-266 and Ser-255, Figure 7.

¹⁸ Kirsch, J. F.; Eichele, G.; Ford, G. C.; Vincent, M. G.; Jansonius, J. N.; Christen, P. *J. Mol. Biol.* **1984**, *174*, 497.

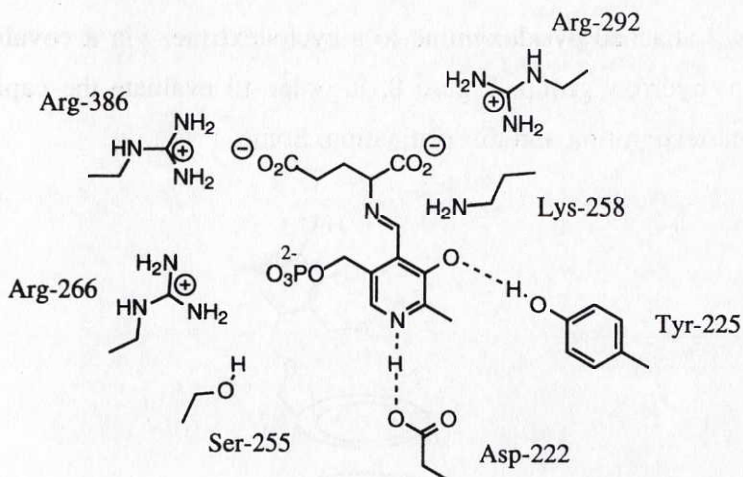


Figure 7. Outline of the active site of aspartate aminotransferase.

The PLP-based enzymatic transamination proceeds via an allylic rearrangement, where the C_{α} -H bond of the amino acid is broken, and a new C-H bond at the 4'-carbon of the cofactor is formed. The proton used in the formation of the new C-H bond is not the same as the one abstracted from the C_{α} -carbon of the substrate.

Non-enzymatic transamination¹⁹ between α -amino acids and α -keto acids can occur in the presence of free cofactor as well as with the holoenzyme, but with much lower reaction rates and selectivities. In many cases metal ions (e.g. Al^{3+}) accelerate the transamination²⁰ reaction through stabilisation of high-energy intermediates. Most model systems that mimic transamination use the pyridoxamine form of the cofactor as the reactant, since the equilibrium constants favour the formation of pyridoxal and α -amino acid.

¹⁹ Martell, A. E. *Acc. Chem. Res.* **1989**, *22*, 115.

²⁰ a) Martell, A. E.; Taylor, P. A. *Inorg. Chim. Acta*, **1988**, *152*, 181.

b) Martin, R. B. *Inorg. Chem.* **1987**, *26*, 2197.

Breslow²¹ attached pyridoxamine to a cyclodextrine, via a covalent bond to the 5'-hydroxy group, Figure 8, in order to evaluate the capacity for substrate recognition and discrimination. Some

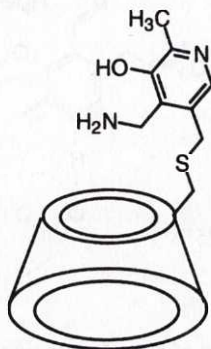


Figure 8. The cyclodextrine derivative used by Breslow.

selectivity was shown for α -keto acids substituted by phenyl and alkylphenyl groups in the α -position. A number of other organic structures have also been attached to pyridoxamines by Breslow and co-workers, and their potential as enzyme mimics evaluated²².

Murakami and co-workers have introduced pyridoxine moieties in vesicle bilayers²³ in an attempt to control the stereochemistry of the reaction. Small, 6-residue, polypeptides functionalised with pyridoxal and

²¹ a) Breslow, R. *Chemica Scripta* **1987**, 27, 555.

b) Breslow, R.; Czarnik, A. W.; Lauer, M.; Leppkes, R.; Winkler, J. Zimmermann, S. C. *J. Am. Chem. Soc.* **1986**, 108, 1969.

c) Breslow, R.; Canary, J. W.; Varney, M.; Waddell, S. T.; Yang, D. *J. Am. Chem. Soc.* **1990**, 112, 5212.

²² a) Breslow, R.; Czarnik, A. W.; Zimmermann, S. C. *J. Am. Chem. Soc.* **1983**, 105, 1694.

b) Breslow, R. *Ann. NY Acad. Sci.* 471 (Int. Symp. Bioorg. Chem, **1985**), 60.

c) Weiner, W.; Winkler, J.; Zimmermann, S. C.; Czarnik, A. W.; Breslow, R. *J. Am. Chem. Soc.* **1985**, 107, 4093.

d) Breslow, R.; Chmielewski, J.; Foley, D.; Johnson, B.; Kumabe, N.; Varney, M.; Mehra, R. *Tetrahedron* **1988**, 44, 5515.

²³ Murakami, Y.; Kikuchi, J.-I.; Akiyoshi, K.; Imori, T. *J. Chem. Soc., Perkin Trans. 2*, **1985**, 1919.

pyridoxamine have been used for transamination studies by Imperiali *et al*²⁴

Wu²⁵ studied the reactivity of a pyridoxamine derivative with an attached propellane designed to function as a bifunctional catalyst, Figure 9. One nitrogen

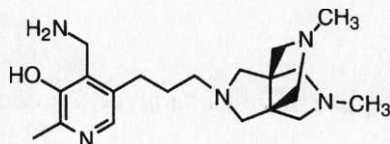


Figure 9. The pyridoxamine derivative employed by Wu.

was expected to abstract a proton and the other was expected to donate a proton. The work by Wu was a thorough investigation of the inter- versus intramolecularity of the proton transfer step in the aldimine-ketimine conversion of the transamination reaction.

The propellane moiety functioned as a bifunctional proton abstractor and donor in the intramolecular transamination reaction, but no rate enhancements were observed, possibly due to coordination of the Zn^{2+} ion to the amine side chain.

These model systems have all provided partial solutions to the problems of achieving reaction rate enhancements, stereoselectivity, and metal coordination but the substrate recognition, solubility, and turnover are problems that have so far not been solved.

²⁴ a) Imperiali, B.; Sinha Roy, R. *J. Org. Chem.* **1995**, *60*, 1891.

b) Imperiali, B.; Sinha Roy, R. *Tetrahedron Lett.* **1996**, *37*, 2129.

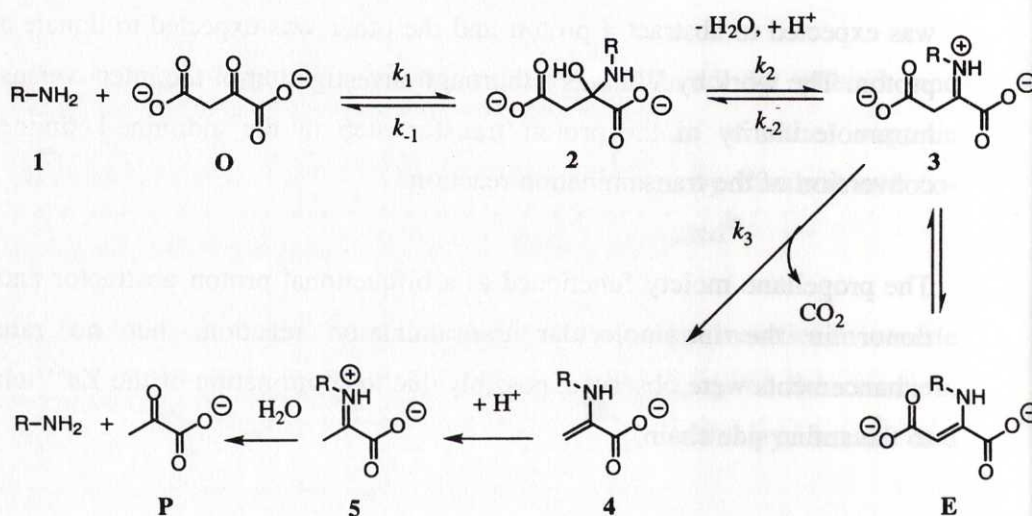
²⁵ a) Wu, Y.-K. Thesis, Göteborg University, **1991**.

b) Wu, Y.-K.; Ahlberg, P. *Acta Chem. Scand.* **1992**, *46*, 60.

2.3 Artificial decarboxylases

The native enzyme oxaloacetate decarboxylase catalyses the decarboxylation of oxaloacetate into pyruvate. It uses a metal ion as cofactor to enhance its catalytic activity. The catalysis of this reaction without the metal ion has been an important goal in mimicking this class of enzymes.

The reported decarboxylase mimics catalyse the decarboxylation through a multi-step amine-catalysed reaction where the species that is decarboxylated is the imine (**3**), Scheme 1²⁶. The first step of the proposed



Scheme 1.

reaction mechanism is the nucleophilic attack of the amine (**1**) nitrogen on the carbonyl group of the substrate (**O**) to form an unstable carbinolamine (**2**) that collapses into a ketimine or Schiff base (**3**). The ketimine, which is the species that loses CO₂, is in equilibrium with the enamine (**E**). After

²⁶ Johansson, K.; Allemann, R. K.; Widmer, H.; Benner, S. A. *Nature* **1993**, 365, 530.

loss of CO_2 , the enamine (4) rearranges to the imine (5), which is hydrolysed to form pyruvate (P) with regeneration of the catalyst (1). The imine/enamine intermediates (3/E and 4/5) on the reaction pathway have been identified by trapping with NaBH_3CN .

The proposed mechanism states that either the formation of carbinolamine from free amine and substrate or the collapse of the carbinolamine into the imine is the rate-determining step of the reaction, whereas the decarboxylation step itself is not. Efficient binding of the substrate would therefore be one of the essential goals in the design of an efficient oxaloacetate decarboxylase mimic.

The amine-catalysed decarboxylation of oxaloacetate has been studied through a variety of model systems in order to design efficient catalysts for the reaction. Pedersen proposed in 1954 that the reaction proceeds through an imine intermediate²⁷. Hay studied the mechanism of aniline-catalysed decarboxylation of oxaloacetate in ethanol and suggested that the formation of the Schiff base is the rate determining step in the reaction²⁸.

In the study of the decarboxylation of oxaloacetate Klotz and co-workers used a modified polyethylenimine where approximately 10% of the nitrogens exists in the form of free primary amines²⁹. This polyimine showed saturation kinetics and a dissociation constant in the range of 10^{-3} M^{-1} as well as a catalytic constant, k_2 , of 2.1 min^{-1} , which when compared to a monomolecular primary amine corresponds to a rate enhancement of approximately five orders of magnitude.

²⁷ Pedersen, K. J. *Acta Chem. Scand.* **1954**, *8*, 710.

²⁸ Hay, R. W. *Aust. J. Chem.* **1965**, *18*, 337.

²⁹ Spetnagel, W. J.; Klotz, I. M. *J. Am. Chem. Soc.* **1976**, *98*, 8199.

substrate to the cationic peptide lowers the free energy barrier of the binding steps of the mechanism, and the imine formation is no longer rate-determining for oxaldie 1, according to the authors.

2.4 *Summary*

The synthesis of complex organic structures with cofactors or specific reactive groups attached as model systems have been used for mimicking enzyme reactions. Rate enhancement, stereoselectivity, and metal ion coordination are problems for which partial solutions have been suggested, while turnover, substrate recognition and discrimination, solubility in aqueous solution are problems that have so far not been solved.

Folded polypeptides have well-defined structures which can be used as scaffolds for the engineering of reactive sites including complementary functional groups for catalysis or recognition. The amino acid sequence of a folded polypeptide can easily be systematically varied in order to optimise a designed reactive site. The structure of folded polypeptides can be determined accurately through modern methods of spectroscopy. Folded polypeptides are large enough to guarantee the solubility in aqueous solution of the model system, which in some reactions is a requirement for turnover. Intermediates on the reaction pathway can be studied through modern spectroscopic means such as NMR spectroscopy. Modern synthetic protocols and HPLC methods make the synthesis and purification of large polypeptides (< 100 residues) a straightforward exercise.

3. Polypeptide design, structure, and reactivity

3.1. Rational design of polypeptides

The interest in *de novo* design of polypeptides with well-defined tertiary structures stems from the importance of protein folding and the interest in the engineering of new proteins with novel functions. The design and study of small polypeptides, with less than 100 residues has enhanced our understanding of the protein folding mechanism. The design of tailor-made proteins that have well-defined tertiary structure and introduce complementary functionalities for catalysis and recognition is now therefore becoming possible. A small number of polypeptides with such properties has been reported. A self-replicating ligase-like 33-residue polypeptide has been reported³², as well as a 31-residue polypeptide that forms parallel four-helix bundles and binds heme units cooperatively³³. KO-42, a 42-residue polypeptide that folds into a helix-loop-helix motif catalyses the hydrolysis and transesterification of *p*-nitrophenyl esters with a rate enhancement over the reaction with 4-methylimidazole of more than three orders of magnitude³⁴.

3.2. Design and structure of SA-42 and RA-42

SA-42³⁵, a polypeptide with 42 amino acid residues, was previously designed to fold into a helix-loop-helix motif and dimerise in solution to form a four-helix bundle. The helical segments were designed using amino acids of high helix propensity^{36,37}. The helices were further

³² Severin, K.; Lee, D. H.; Kennan, A. J.; Ghadiri, M. R. *Nature* **1997**, *389*, 706.

³³ Rabanal, F.; DeGrado, W. F.; Dutton, P. L. *J. Am. Chem. Soc.* **1996**, *118*, 473.

³⁴ Broo, K. S.; Brive, L.; Ahlberg, P.; Baltzer, L. *J. Am. Chem. Soc.* **1997**, *119*, 11362.

³⁵ Olofsson, S., Thesis, Göteborg University, **1994**.

³⁶ O'Neil, K. T.; DeGrado, W. F. *Science*, **1990**, *250*, 669.

³⁷ Chou, P.Y.; Fasman, G. D. *Biochemistry*, **1974**, *13*, 222.

stabilised through helical dipole stabilisation³⁸, capping, and salt bridge formation. A loop between the two helical segments was introduced using amino acids with helix-breaking properties so that the peptide could fold into a hairpin motif driven by the hydrophobic interactions between amphiphilic helices³⁹. The hydrophobic core of SA-42 contains phenylalanine, leucine, isoleucine and norleucine residues. The amino acid sequence was varied and included 16 different amino acids, to facilitate structural investigation and resonance assignments by NMR spectroscopy. Two phenylalanine residues were placed at the lower end of helix II, to induce chemical shift dispersion and function as NOE reporter groups. Studies of SA-42 in solution by NMR and CD spectroscopy as well as by ultracentrifugation revealed that it does form an amphiphilic helix-loop-helix motif that dimerises in an antiparallel fashion.

The SA-42 sequence was modified in order to design the polypeptide catalyst RA-42, a 42-residue peptide which performs acyl transfer reactions of activated esters⁴⁰. The structure of RA-42 is similar to that of SA-42, and a reactive site was introduced. The reactive site of RA-42 was designed with a histidine residue at position *i* (His-11) and an ornithine residue in position *i*+4 (Orn-15), Figure 11.

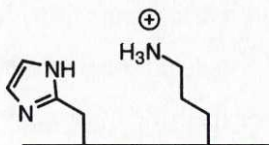


Figure 11. Schematic representation of the reactive site of RA-42.

³⁸ Hol, W. G. J.; van Duijnen, P. T.; Berendsen, H. J. C. *Nature*, **1978**, 273, 443.

³⁹ a) Kellis, Jr. J. T.; Nyberg, K.; Sali, D.; Fersht, A. R. *Nature*, **1988**, 333, 784.

b) Chotia, C. *Nature*, **1974**, 248, 338.

⁴⁰ a) Baltzer, L.; Lundh, A.-C.; Broo, K.; Olofsson, S.; Ahlberg, P. *J. Chem. Soc., Perkin Trans. 2* **1996**, 1671.

b) Lundh, A.-C.; Broo, K.; Baltzer, L. *J. Chem. Soc., Perkin Trans. 2* **1997**, 209.

The purpose of the design was to obtain a reactive centre with a nucleophilic catalyst, the imidazolyl group of the histidine, and a flanking positively charged hydrogen bond donor that could bind one or both of the oxygens in the developing oxyanion in the transition state of the acyl-transfer reaction.

3.3 The reactivity of RA-42

RA-42 was reacted with mono-*p*-nitrophenyl fumarate in 10 % TFE at pH 5.85 and 293 K under the release of *p*-nitrophenol with a second-order rate constant of $28 \cdot 10^{-3} \text{ M}^{-1} \text{ s}^{-1}$ which is 8.3 times larger than the second-order rate constant of the 4-methyl-imidazole catalysed reaction, $3.38 \cdot 10^{-3} \text{ M}^{-1} \text{ s}^{-1}$. The reaction was studied over a wide pH range, in order to identify the reactive residues, and the pH profile of the reaction showed that the histidine was the catalytically active amino acid. The reaction products were identified by NMR spectroscopy and mass spectroscopy and it was found that the acyl group of the substrate formed an amide of the side chain of an Orn or a Lys residue. The results showed that the reaction proceeded via an initial and rate determining formation of an acyl intermediate under the release of *p*-nitrophenol, followed by a fast intramolecular transfer of the acyl group to the side chain of the flanking ornithine residue. The discovered reaction has been shown to be a convenient method for the site-selective introduction of new functionalities into folded polypeptide systems.

3.4. The site selectivity of RA-42

There are three residues in RA-42 with side chains that can form amide bonds, Orn-15, Lys-19 and Orn-34. Broo established by trypsin-catalysed cleavage of the acylated peptide and identification of the fragments by ES-

MS that in RA-42 one equivalent of fumarate acylates only Orn-15⁴¹, and the reaction was found to be site-selective. Only residues in position $i+4$ or $i-3$ relative to the histidine in position i are amidated.

The proposed reaction sequence for the acyl transfer reaction is shown in Figure 12.

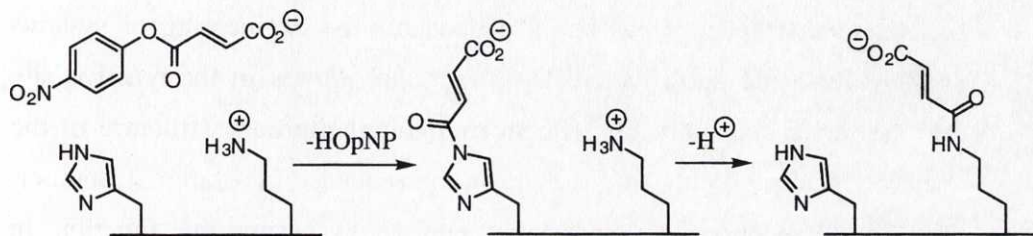


Figure 12. Proposed reaction sequence for the acyl transfer reaction of RA-42.

⁴¹ Broo, K.; Allert, M.; Andersson, L.; Erlandsson, P.; Stenhagen, G.; Wigström, J.; Ahlberg, P.; Baltzer, L. *J. Chem. Soc. Perkin Trans. 2* **1997**, 397.

4. Folded polypeptide model systems

The active site of native enzyme is commonly a hydrophobic crevice made up of a large number of amino acid residues, that can bind the substrate and the transition state. Folded polypeptides have sufficient size and complexity to be used as templates for the engineering of enzyme mimics. On the surface of the folded motif reactive sites can be built, where complementary groups can be introduced for the engineering of systems with tailor-made specificities. The functional groups in the reactive site can be varied systematically without changing the tertiary structure of the peptide by changing the amino acids in the sequence in a rational manner. Folded polypeptides are also large enough to ensure the function in aqueous solutions of groups that are normally not soluble in water, such as the reduced or oxidised forms of cofactor model systems. Polypeptide chemistry utilises standardised synthesis protocols that have been automatized and allows the efficient synthesis of large amounts of peptides in high yields.

This thesis describes the design and synthesis of folded polypeptide model systems for the study of NAD^+/NADH reactions, transamination, and decarboxylation reactions. The site-selective functionalisation reaction has been used to incorporate a cofactor mimic into a folded polypeptide template to form a model system. Non-covalent control of site-selective functionalisation has also been used to incorporate a cofactor into a folded polypeptide system.

5. The preparation of a NAD⁺/NADH model system by post-synthetic modification of a folded polypeptide: RA-42NAD and LA-42NAD

5.1 The structure of RA-42

RA-42 is a 42-residue polypeptide that folds into a helix-loop-helix motif and dimerises in solution into an antiparallel four-helix bundle. The reactive site of RA-42 consists of His-11 and Orn-15 and it reacts rapidly and site-selectively with mono-*p*-nitrophenyl fumarate, to form an amide bond at the side chain of the ornithine residue⁴¹. A NAD⁺/NADH mimicking model system has been prepared by the site-selective incorporation of a nicotinoyl residue into RA-42 with the purpose of creating a catalyst that is water soluble in both redox forms and where the reactive site can be supplemented with residues that provide enhanced reactivity and selectivity.

The solution structure of RA-42 has been determined by TOCSY and NOESY ¹H NMR experiments, and by CD spectroscopy⁴⁰. The amino acid sequence of RA-42 is shown in Figure 13, with residues making up the reactive site underscored

Asn-Aib-Ala-Asp-Nle-Glu-Ala-Ala-Ile-Lys- <u>His</u> -Leu-Ala-Glu- <u>Orn</u> -Nle-Aib-Ala-Lys-	11	15	19
			Gly-Val-Pro-Asp
			20 23
Gly-Aib-Arg-Ala-Phe-Ala-Glu-Phe-Orn-Lys-Ala-Leu-Gln-Glu-Ala-Nle-Gln-Ala-Aib			24
42			

Figure 13. The amino acid sequence of RA-42 with the residues that form the reactive site underscored.

LA-42 is a 42-residue polypeptide which is identical to RA-42 except that Orn-15 has been replaced by a lysine. The substitution resulted in a slight increase in reactivity towards mono-*p*-nitrophenyl fumarate.

5.2 Synthesis of the NAD⁺ cofactor mimics

In order to incorporate a NAD⁺ model compound site-selectively into RA-42 a nicotinoyl compound in the form of an activated ester was required and the *p*-nitrophenyl ester of *N*-methylnicotinic acid iodide, **2**, Figure 14, was prepared through esterification of nicotinic acid with

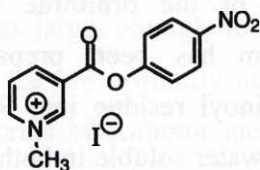


Figure 14. The *p*-nitrophenyl ester of *N*-methylnicotinic acid iodide, **2**.

p-nitrophenol using DCC and pyrrolidinopyridine as coupling reagents⁴², after which the ester was methylated with methyl iodide in DMF. The product was used both for the incorporation into the peptides RA-42 and LA-42 and as a reagent in the synthesis of **3**, Figure 15.

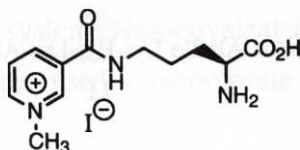


Figure 15. N_ε-(*N*-methylnicotinoyl)-L-ornithine iodide, **3**.

Compound **3** was prepared by first making a copper chelate of L-ornithine and then adding the *p*-nitrophenyl ester **2** to the chelate.

⁴² Hassner, A.; Alexanian, V. *Tetrahedron Lett.* **1978**, 4475.

Compound **3** and 1-methylnicotinamide were used for comparison of the rate of reduction and of the stability of the reduced form of the NAD⁺ species with the that of the peptide bound model system.

5.3 Incorporation of the NAD⁺ cofactor mimic into RA-42 and LA-42

The nicotinoyl moiety was incorporated into RA-42 in a one-step reaction in aqueous solution at pH 5.9 by treatment of a peptide solution (0.8 mM in 50 mM NaOAc buffer) with a tenfold excess of the *p*-nitrophenyl ester. The release of *p*-nitrophenol was monitored spectrophotometrically at 340 nm.

For the preparative incorporation experiments LA-42 was used instead of RA-42 due to its slightly higher reactivity.

The second-order rate constant for the reaction between 4-methylimidazole (4-MeIm) and **2** was $5.5 \cdot 10^{-3} \text{ M}^{-1} \text{ s}^{-1}$ and the background hydrolysis proceeds with a pseudo first-order rate constant of $3.17 \cdot 10^{-4} \text{ s}^{-1}$. As the reactivity of LA-42 is approximately five times higher than that of 4-MeIm in aqueous solution the estimated second-order rate constant of the LA-42 catalysed reaction is $2.75 \cdot 10^{-2} \text{ M}^{-1} \text{ s}^{-1}$. For a 0.8 mM solution of LA-42 the pseudo first-order rate constant becomes $2.2 \cdot 10^{-5} \text{ M}^{-1} \text{ s}^{-1}$ and the ratio of the pseudo first-order rate constants of the peptide catalysed and the background reaction is such that approximately 7% of the ester will react with the peptide, whereas 93% will be hydrolysed. As the reaction proceeds the concentration of reactive LA-42 is diminished and therefore also the rate of incorporation. The reaction was thus carried out in two steps and the amount of functionalised peptide determined by ES-MS after each step.

In the first incorporation 6 mg, a thirteenfold excess, of the ester **2** was added to a solution of 5.2 mg of LA-42 (0.8 mM) in aqueous solution (1.5 mL, NaOAc 50 mM) at pH 5.9. The incorporation was followed by UV spectroscopy at 340 nm, by monitoring the release of *p*-nitrophenol. The reaction mixture was analysed by LC-ESMS and the transformed spectrum showed one peak at mass 4509.35 corresponding to the mass of LA-42 (4390.10) and 1-methylnicotinic acid (138.20) less that of water (18.02) and a second peak at the mass of LA-42 (4390.10) with no trace of a diacylated product. The ratio of the intensities indicated that approximately 60-70% of LA-42 had been acylated in the reaction and the concentration of unmodified LA-42 was therefore approximately 0.24 mM.

LA-42 was then treated with 8 mg of **2**, a sixtyfold excess, where the excess amount was again estimated from the ratio between the pseudo first-order rate constants of the LA-42 catalysed reaction and that of the background reaction. It was approximately 50, since only a fraction of the peptide LA-42 remained non-acylated. LA-42NAD was obtained in a yield of 4.2 mg, which is better than 70% based on the amount of LA-42 used as starting material.

5.4 The structure of LA-42NAD

The mean residue ellipticity of LA-42NAD was $-18\ 500\ \text{deg cm}^2\ \text{dmol}^{-1}$, which is the same as that of RA-42 within the experimental error limits, suggesting that the folds are the same. The peptide NAD⁺ model was also studied by ¹H NMR spectroscopy. The nicotinoyl ring has four protons that make up a coupled spin system, Figure 16, and in the TOCSY experiment this spin system



Figure 16. The spin system in the nicotinoyl residues.

is readily observed. The TOCSY spectrum, however, showed three different nicotinoyl spin systems, one with sharp resonances of high intensity and two spin systems with line width similar to those of the peptide resonances. The former spin system was assigned to free N-methyl nicotinic acid and the latter two to peptide-bound nicotinoyl residues. The fact that the two polypeptide-bound spin systems are observed is probably due to the *cis-trans* equilibrium of the functionalised amide. The successful site-selective incorporation of a NAD^+ model into the folded polypeptide LA-42 has thus been shown.

5.5 Reduction of LA-42NAD into LA-42NADH

LA-42NAD was treated with a tenfold excess of sodium dithionite and sodium carbonate (1:1) in aqueous solution at pH 7 under a nitrogen atmosphere and the formation of the desired 1,4-dihydro species was monitored spectrophotometrically at 360 nm. LA-42NADH had a half-life greater than the corresponding reduced form of free 1-methyl nicotinamide by at least a factor of three, see Figure 17. The reduced

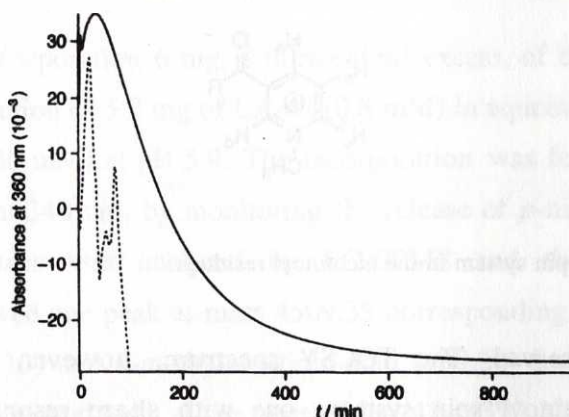


Figure 17. UV absorbance at 360 nm of LA-42NAD and 1-methylnicotinamide in arbitrary units as a function of time.

form of the free cofactor also precipitates in the cuvette, thereby causing the jagged appearance of the spectrum. LA-42NAD is completely soluble throughout the reduction sequence.

LA-42NAD was also treated with a tenfold excess of sodium dithionite and sodium carbonate (1:1, 90:10 H₂O:D₂O, pH 7) in 5 % (v/v) trifluoroethanol (TFE) in 90:10 H₂O:D₂O at pH 7 under a nitrogen atmosphere and studied by ¹H NMR spectroscopy. The 1D ¹H NMR spectrum showed resonances from three different nicotinoyl residues, the sharp resonances were assigned to the free N-methyl nicotinic acid and the broadened resonances were assigned to the two rotamers of the peptide-bound nicotinoyl moiety, Figure 18. After addition

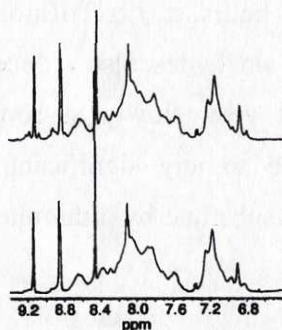


Figure 18. Part of the ^1H NMR spectrum of LA-42NAD showing the reduction of the incorporated nicotinoyl residue by sodium dithionite. The top trace shows the spectrum before reduction and the broadened resonances at 9.19, 8.94 and 8.72 ppm that were assigned to the peptide-bound NAD^+ model are unaffected. The bottom trace shows the spectrum after nearly complete reduction and the intensity of these resonances have decreased markedly.

of the sodium dithionite/sodium carbonate mixture the intensities of the broadened resonances decreased and finally disappeared, whereas the sharp resonances were virtually unaffected.

The NAD^+ model was therefore successfully reduced and it was shown to be water soluble in both the oxidised and the reduced form. The stability of the reduced form was enhanced by incorporation into the folded peptide.

5.6 Reduction of α,α,α -trifluoro acetophenone using LA-42NADH

To test whether the NADH model system could catalyse the reduction of a carbonyl compound LA-42NAD was treated with a tenfold excess of sodium dithionite and sodium carbonate (1:1) in 5 % (v/v) trifluoroethanol (TFE) at pH 7 under a nitrogen atmosphere and a tenfold

excess of α,α,α -trifluoro acetophenone was added. The reaction was followed by ^{19}F NMR for 36 hours. α,α,α -Trifluoro acetophenone is, like many unhindered ketones or aldehydes, also reduced by sodium dithionite in aqueous solutions, albeit very slowly at room temperature⁴³. LA-42NADH did not give rise to any significant reduction beyond the background reduction of the substrate by dithionite.

5.7 Summary

The incorporation of the NAD^+ cofactor model into LA-42 was verified through LC-ESMS and 2D ^1H NMR. It has been shown, using CD and 2D ^1H NMR spectroscopy, that the incorporation of the cofactor into the folded peptide does not adversely effect the structure of the polypeptide motif. The reduction of the NAD^+ analogue was accomplished and verified by UV spectroscopy and ^1H NMR. The incorporated and reduced cofactor has a lifetime that exceeds the lifetime of the free 1-methylnicotinamide by at least a factor of three. Both the *ox.* and the *red.* form of the peptide-bound cofactor model are soluble in water. Attempts to reduce an activated substrate did not, so far, show any reaction enhancement over the background reaction.

⁴³ a) de Vries, J. G.; van Bergen, T. J.; Kellog, R. M. *Synthesis*, 1977, 246.

b) de Vries, J. G.; Kellog, R. M. *J. Org. Chem.* 1980, 45, 4126.

6. Non-covalent control of site-selective incorporation: PP-42 and pyridoxal phosphate

6.1 The design of PP-42

In the enzyme catalysed transamination reaction pyridoxal phosphate (PLP) forms an internal aldimine with a lysine side chain in the active site after which the amino group of the substrate replaces the lysine side chain in an exchange reaction. In order to develop a model system for the study of the enzyme-like transamination, PP-42 has been designed to mimic key steps in the catalytic cycle and to catalyse transaminase-like reactions. To mimic the first step PP-42 was designed to react with the cofactor and form an aldimine at the side chain of a lysine residue and to control the site-selectivity of the incorporation through interactions between the phosphate group of PLP and an arginine residue in the reactive site.

The design of PP-42 is based on that of RA-42 with only minor changes in the amino acid sequence. The reactive site was designed with three lysine residues in positions 11, 15, and 30, one histidine at position 7, and two arginines in positions 10 and 19, Figure 19.

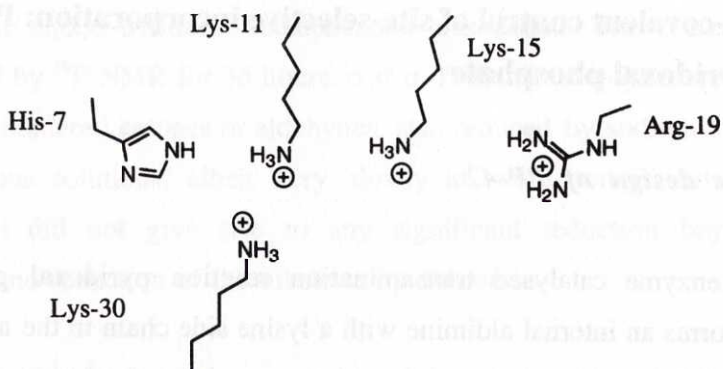


Figure 19. Schematic representation of the reactive site of PP-42.

The reactive site was loosely modelled after the active site of aspartate aminotransferase¹⁸, with two 'extra' lysine residues, at positions 15 and 30, introduced to enhance the possibility of having one lysine in an optimum position to function as base in the proton transfer reaction. The arginine residues were included to bind pyridoxal phosphate.

The Aib residues used in the sequences of SA-42 and RA-42 were replaced by alanines, and the amino acid sequence of PP-42 is shown in Figure 20, with the amino acid residues of the reactive site underscored.

Asn-Ala-Ala-Asp-Nle-Glu- <u>His</u> -Ala-Ile-Arg- <u>Lys</u> -Leu-Ala-Glu- <u>Lys</u> -Nle-Ala-Ala- <u>Arg</u> -				
1	7	11	15	19
			-Gly-Pro-Val-Asp-	
			20	23
Gly-Ala-Arg-Ala-Phe-Ala-Glu-Phe-Glu-Arg-Ala-Leu- <u>Lys</u> -Glu-Ala-Nle-Gln-Ala-Ala				
42		30		24

Figure 20. The amino acid sequence of PP-42 with the residues that form the reactive site underscored.

6.2. The structure of PP-42

PP-42 was prepared and purified using standard Fmoc protocols and HPLC and it was identified from the LC-ESMS spectrum where a fragment of mass 4531.5, corresponding to the weight of PP-42, was detected. The mean residue ellipticity of PP-42 at 222 nm at a concentration of 0.60 mM and pH 7.0 is $-24\,500 \pm 1000 \text{ deg cm}^2 \text{ dmol}^{-1}$, a value that is comparable to those of other designed helix-loop-helix dimers and more negative than that of RA-42. A schematic representation of PP-42 is shown in Figure 21.

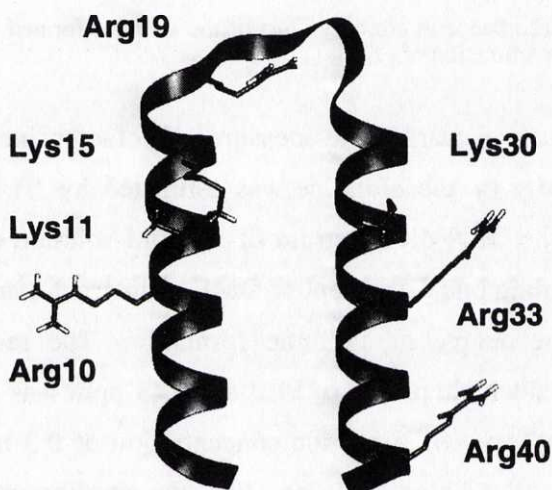


Figure 21. Schematic representation of PP-42. Only the side chains of the residues which might influence the incorporation of PLP are shown.

6.3 Incorporation of pyridoxal phosphate into PP-42

The incorporation of pyridoxal phosphate into PP-42 in aqueous solution and room temperature was demonstrated by UV spectroscopy, by monitoring the appearance and growth of the aldimine absorbance at 389

nm. A pH profile of the absorbance was also obtained where the optimum pH for incorporation was found to be 4.4, Figure 22.

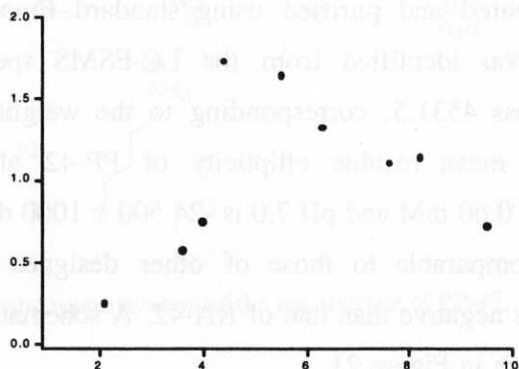


Figure 22. UV absorbance in arbitrary units of the aldimine formed between PLP and PP-42 at 389 nm as a function of pH.

In order to obtain a quantitative measure of cofactor incorporation the molar absorptivity of the aldimine was estimated by ^1H NMR and UV spectroscopy. The ^1H NMR spectrum of a 1 mM solution of PLP in D_2O at pH 4.4 containing one equivalent of DMF as internal standard was used to determine the degree of aldimine formation. The reduction of the intensity of the aldehyde proton of PLP at 10.43 ppm was measured after addition of PP-42 to a final peptide concentration of 0.3 mM. Under the assumption that PP-42 binds only one PLP the equilibrium concentration of aldimine, PLP, and PP-42 could be calculated and the molar absorptivity was calculated from the aldimine absorbance at 389 nm to be approximately $4000 \text{ M}^{-1} \text{ cm}^{-1}$.

For the study of transamination reactions with PLP-functionalised PP-42 it was necessary to optimise the fraction of incorporated cofactor. An aqueous solution of PP-42 at pH 4.4 was treated with a fivefold excess of PLP and the degree of functionalisation was determined by UV

spectroscopy to be greater than 95%. The degree of incorporation was also studied by LC-ESMS and the transformed mass spectrum of the equilibrium solution showed the presence of one peak at 4761.3 (mass of PP-42 (4531.5) plus mass of PLP (247.2) less the mass of water (18.02)) and one peak at 4531.5 (mass of PP-42). The ratios of the intensities of the two peaks indicated that approximately 25% of the peptide had been functionalised. As the HPLC treatment of the sample shifts the equilibrium towards free PLP and free PP-42, a more reliable measure of the degree of incorporation was needed. The aldimine bond was therefore reduced to form a secondary amine before the peptide was subjected to LC-ESMS analysis.

Upon reduction of the aldimine group by alkaline NaBH_4 ⁴⁴ the absorbance at 389 nm disappeared. Instead an absorbance at 290 nm appeared, which was assigned to the reduced functionalised peptide⁴⁵. The reduced PP-42-PLP was analysed with LC-ESMS and the transformed spectrum showed a peak at 4764.56 (mass of PP-42 (4533.6) plus mass of PLP (247.2) plus the mass of 2H (2.02) less the mass of water (18.02)) and one peak at 4533.6 (mass of PP-42). The ratios of the intensities of the two peaks indicated that approximately 75% of the peptide had been functionalised. No difunctionalised peptide was observed in the mass spectrum.

In order to determine the site of incorporation the reduced functionalised peptide was digested with trypsin, which cleaves peptide bonds on the C-terminal side of unhindered lysine and arginine residues. The trypsin cleavage sites in the amino acid sequence of unreacted PP-42 are shown in Figure 23, with the relevant residues in boldface.

⁴⁴ Paine, L. J.; Perry, N.; Popplewell, A. G.; Gore, M. G.; Atkinson, T. *Biochim. Biophys. Acta* **1993**, *1202*, 235.

⁴⁵ Lo Bello, M.; Petruzelli, R.; Reale, L.; Ricci, G.; Barra, D.; Federici, G. *Biochim. Biophys. Acta* **1992**, *1121*, 167.

Asn-Ala-Ala-Asp-Nle-Glu-His-Ala-Ile- Arg -Lys-Leu-Ala-Glu- Lys -Nle-Ala-Ala- Arg -				
1	7	11	15	19
				-Gly-Pro-Val-Asp-
			20	23
Gly-Ala- Arg -Ala-Phe-Ala-Glu-Phe-Glu- Arg -Ala-Leu- Lys -Glu-Ala-Nle-Gln-Ala-Ala				
42	34	30		24

Figure 23. Amino acid sequence of PP-42 with trypsin cleavage sites in boldface.

The digested polypeptide was analysed by LC-ESMS and one peak in the transformed mass spectrum (1669.8) that corresponds to the fragment of the Gly-20 to Arg-33 sequence (1438.64) plus the mass of PLP (247.2) and 2H (2.02) less the mass of water (18.02) was found. This fragment accounted for approximately 85% of the functionalised peptide in the mass spectrum. A minor amount of incorporation of the cofactor at the side chain of Lys-11 was also observed. The proximity of Arg-19 to Lys-30 in the reactive site is apparently enough to control the functionalization of the side chain of the lysine, Figure 24. Arg-10 is similarly

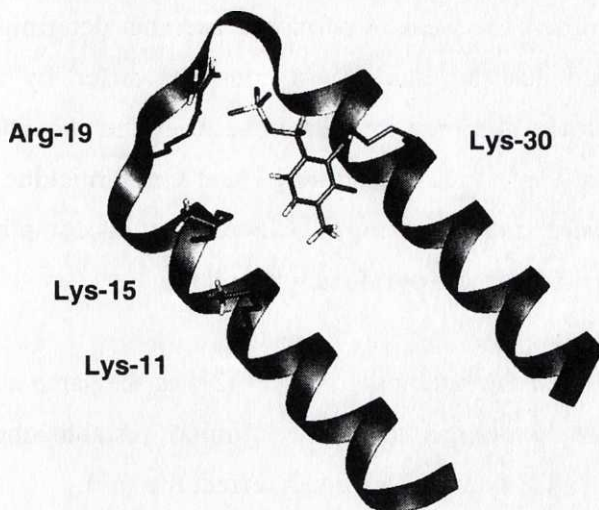


Figure 24. Schematic representation of PP-42 with the aldimine between Lys-30 and PLP shown. Also shown are the positions of Arg-19, Lys-11 and Lys-15.

in proximity to Lys-11 in a helical conformation and appears to give rise to small amounts of aldimine formation too, under conditions of excess PLP over peptide. Lys-15 is not flanked by an arginine residue and does not form any detectable amounts of aldimine with PLP. Arg-19 binding of the phosphate group of PLP apparently controls aldimine formation and the positioning of Arg-19 relative to Lys-30 makes Lys-30 compete favourably with the other lysine residues in PP-42. The positioning of an Arg-Lys pair in a similar two-residue site is therefore likely to be sufficient to ensure the site-selective incorporation of the cofactor in the presence of other lysine residues.

In a control experiment, an aqueous solution of PP-42 was treated with a fivefold excess of pyridoxal hydrochloride under conditions identical to those for the incorporation of PLP. Pyridoxal lacks the phosphate group of PLP and no significant amount of aldimine absorbance was observed in the UV spectrum. The ratio of the absorbances of the two aldimines is difficult to calculate exactly as the aldimine absorbance of the pyridoxal

containing mixture is too weak to permit an accurate determination, but it can be estimated that the equilibrium constants differ by at least two orders of magnitude. A strong interaction between the phosphate group of PLP and the peptide is thus demonstrated and the mimicking of the first step in enzymatic transamination has been now accomplished in the reaction between PP-42 and pyridoxal phosphate.

The CD spectrum of the functionalised PP-42 was the same as that of PP-42 within the experimental error limits, establishing that the incorporation of PLP does not adversely effect the fold.

6.4 An attempted transamination between glutamic acid and pyridoxal phosphate

In order to investigate the ability of PP-42 to catalyse transamination reactions PP-42 was treated with a five-fold excess of PLP in aqueous solution, and the pH was adjusted to 7 in order to minimise the background transamination catalysed by free PLP. A 26-fold excess of L-glutamic acid was added, and the decrease of the aldimine absorbance at 389 nm and the increase in pyridoxamine absorbance at 325 nm was monitored spectrophotometrically over several weeks, Figure 25.

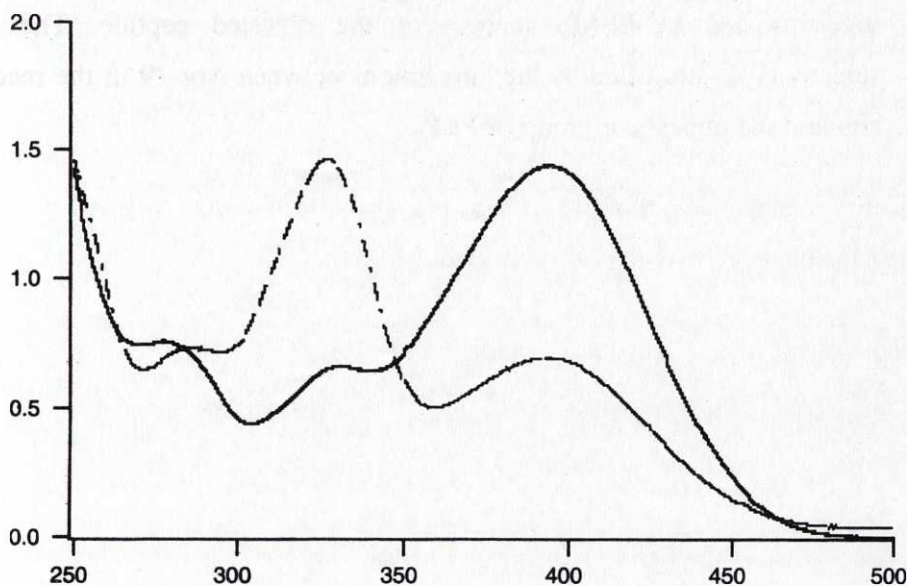


Figure 25. UV spectrum of the transamination reaction involving PP-42 and PLP. The solid line represents the initial spectrum and the dashed line represents the final spectrum after 26 days.

In comparison to a control experiment which was carried out simultaneously under identical conditions but without PP-42 the reaction in the presence of PP-42 proceeded at a slightly slower rate suggesting that the PP-42 bound PLP is inactive and that the concentration of active PLP is therefore reduced in the presence of PP-42. Further developments of the design of PP-42 to enable the reactive site to bind also the aldimine formed from PLP and an amino acid are under way.

6.5 Summary

PP-42 is a folded polypeptide which reacts with PLP to form an aldimine between the cofactor and a lysine residue in the reactive site of the peptide. The site-selectivity of the incorporation of PLP into PP-42 has been demonstrated by reduction of the aldimine bond followed by trypsin

digestion and LC-ESMS analysis of the digested peptide. The site-selectivity is controlled by the interactions between Arg-19 in the reactive site and the phosphate group of PLP.

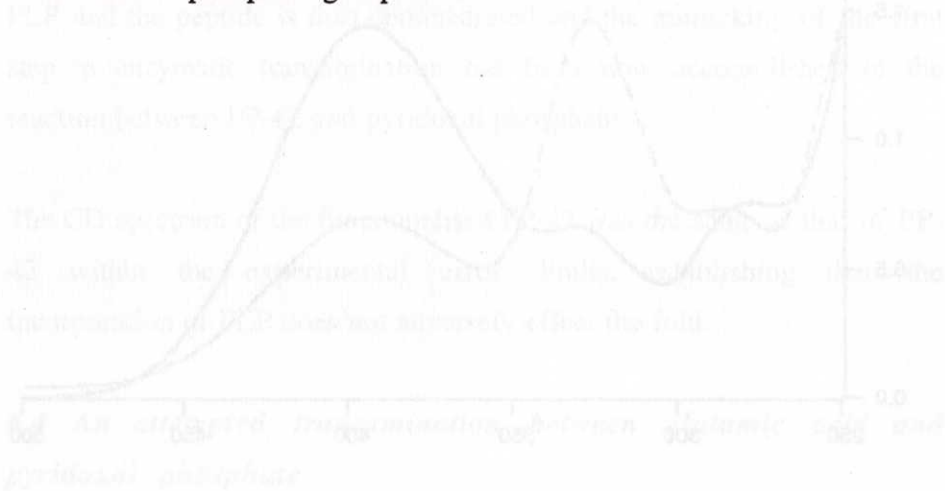


Figure 12. UV spectra of the benzoylation reaction involving TP-42 and PLP. The solid line represents the initial spectrum and the dashed line represents the final spectrum. The increase in PLP absorbance at 280 nm is a clear sign of PLP activation. In comparison to a control experiment which was carried out simultaneously under identical conditions but without TP-42 the reaction in the presence of TP-42 proceeded at a slightly slower rate suggesting that the TP-42 bound PLP is inactive and that the concentration of active PLP is therefore reduced in the presence of TP-42. Further development of the design of TP-42 to enable the reactive site to bind also the aldehyde formed from PLP and an amino acid was under way.

4.3 Summary

TP-42 is a folded polypeptide which reacts with PLP to form an aldehyde between the carbonyl and a lysine residue in the reactive site of the peptide. The site-selectivity of the incorporation of PLP into TP-42 has been demonstrated by reduction of the aldehyde bond followed by trypan

7. Catalysis of the decarboxylation of oxaloacetate: NP-42

7.1 Design of NP-42

In the amine catalysed decarboxylation of oxaloacetate the reaction proceeds via a Schiff base formed between the amine and the substrate. The imine formation has been shown to be the rate-determining step of the reaction. In order to develop a catalyst for the decarboxylation of oxaloacetate NP-42 has been designed to react with oxaloacetate to form an imine in the reactive site and catalyse its decarboxylation.

NP-42 is a 42-residue polypeptide designed to fold into a helix-loop-helix motif and dimerise in solution to form a four-helix bundle. The design of NP-42 is based on the structure of RA-42. It forms a similar hydrophobic core and the NOE reporter groups are the same. Only minor changes were made in the amino acid sequence. A lysine was introduced at position 11 to provide the primary amine functional group and three arginine residues were included to bind the dianionic substrate. The amino acid sequence of NP-42 is shown in Figure 26, with residues in the reactive site underscored.

Asn-Ala-Ala-Asp-Nle-Glu-His-Ala-Ile-Arg- <u>Lys</u> -Leu-Ala-Glu- <u>Arg</u> -Nle-Ala-Ala-Gly-				
1	7	11	15	19
			-Gly-Pro-Val-Asp-	
			20	23
Gly-Ala-Arg-Ala-Phe-Ala-Glu-Phe- <u>Arg</u> -Arg-Ala-Leu- <u>Arg</u> -Glu-Ala-Nle-Gln-Ala-Ala				
42	34	30		24

Figure 26. The amino acid sequence of NP-42 with the residues that form the reactive site underscored.

The reactivity of a primary amine towards oxaloacetate increases as its pK_a decreases. One way to depress the pK_a of an amine such as the ϵ -amino group of a lysine residue is to surround it with several positively charged groups and in the reactive site of NP-42, the single lysine residue is surrounded by three arginine residues. A schematic representation of the reactive site of NP-42 is shown in Figure 27.

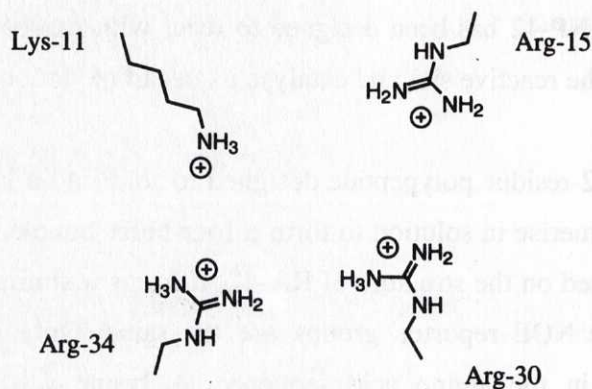


Figure 27. Schematic representation of the designed reactive site of NP-42.

7.2 The structure of NP-42

NP-42 was synthesised and purified using standard Fmoc methods and HPLC and it was identified from the LC-ESMS spectrum where a peptide of mass 4515.98, the weight of NP-42, was detected. The concentration and pH dependence of its helical content was determined by CD spectroscopy. The mean residue ellipticity at 222 nm of NP-42 at 0.5 mM and pH 7 is $-22\ 300 \pm 1000$ deg cm^2 $dmol^{-1}$, which is consistent with that of a folded helix-loop-helix motif. The CD spectrum of NP-42 is pH independent in the range from 4 to 8. The concentration dependence of

the CD spectrum of NP-42 strongly indicates that it forms dimers in solution at concentrations above 0.2 mM, Figure 28.

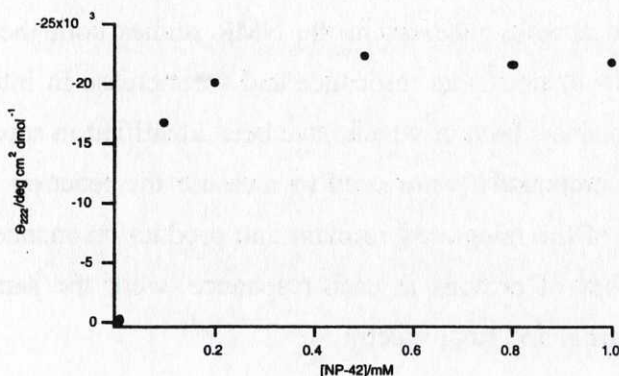


Figure 28. Θ_{222} of NP-42 as a function of the peptide concentration.

The decrease of the absolute value of Θ_{222} below a concentration of 0.2 mM shows that the peptide dimer dissociates into monomers at low concentration. The loss of helical structure affects the reactivity of NP-42 adversely and the practical limit for studies at low concentration is therefore 0.2 mM.

7.3 The NP-42 catalysed decarboxylation of oxaloacetate

The studies of the decarboxylation of oxaloacetate by UV spectroscopy necessitates the use of an estimated molar absorptivity since the reactant or product cannot be directly or separately observed under reaction conditions. The use of ¹H NMR spectroscopy allows the direct observation of both the reactant and the product and uncertainty with regards to which species is actually studied is thus avoided.

In order to demonstrate the catalytic ability of the model system, NP-42 was mixed with a 25-fold excess of oxaloacetate in aqueous solution at pH

7 and the decarboxylation of oxaloacetate was monitored over time using both NMR and UV spectroscopy at 285 nm. The UV measurements monitor the disappearance of oxaloacetate at the wavelength where pyruvate also absorbs whereas in the NMR studies both the decrease in intensity of the oxaloacetate resonance and the increase in intensity of the pyruvate resonance, both of which have been identified in separate spectra of the pure compounds, were used to measure the reaction rate, Figure 29. The sum of the integrated reactant and product resonances, corrected for the number of protons in each resonance, were the same to within 95% in the initial and final spectra.

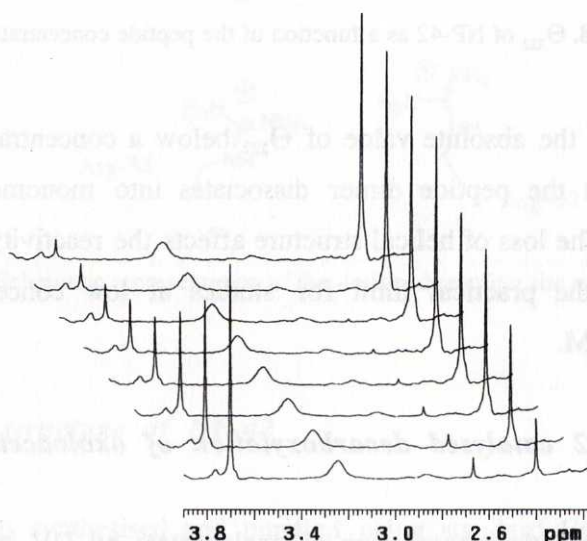


Figure 29. Part of the ¹H NMR spectrum of the reaction mixture of NP-42 and oxaloacetate. The bottom trace shows the reactant oxaloacetate resonance at 3.71 ppm and the product pyruvate resonance at 2.41 ppm. The upper traces are shown in order of increasing reaction time.

The oxaloacetate resonance disappears exponentially with time and a single exponential function could be fitted to the experimental results, Figure 30,

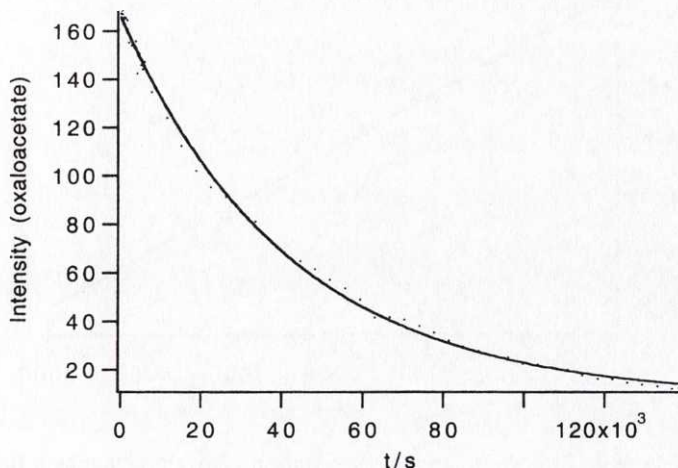


Figure 30. The intensity of the oxaloacetate ^1H NMR resonance in arbitrary units as a function of time.

and the peptide-catalysed decarboxylation can therefore be treated as a pseudo first-order reaction. The same conclusions can be reached after analysis of the exponential increase of the intensity of the pyruvate resonance. The pseudo first-order rate constants of the reaction were determined from initial rates and no saturation kinetics were observed even for a 150-fold excess of substrate over catalyst. A plot of the initial decrease in the concentration of oxaloacetate as a function of time is shown in Figure 31.

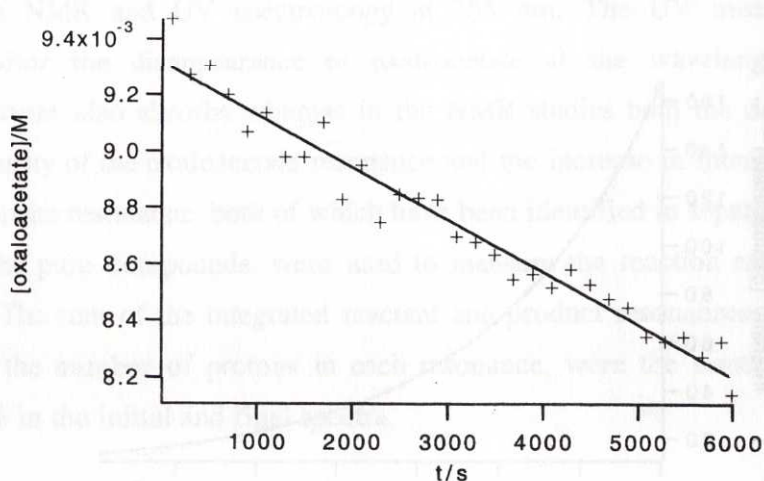


Figure 31. Sample plot of the decrease in concentration of oxaloacetate as a function of time from ^1H NMR resonance intensities of oxaloacetate.

Since the peptide-catalysed decarboxylation reaction does not follow saturation kinetics it can be treated as a bimolecular reaction which follows the second-order rate law:

$$-\frac{d[\text{OAA}]}{dt} = (k_2 \times [\text{NP42}] + k_0) \times [\text{OAA}]$$

where k_2 is the second-order rate constant of the peptide catalysed reaction, and k_0 is the first-order rate constant of the background reaction.

From measurements of the initial rates of the reaction at constant substrate concentration and varied concentration of the peptide catalyst, the pseudo first-order rate constants were obtained and plotted versus the peptide concentration to obtain the second-order rate constants, Figure 32.

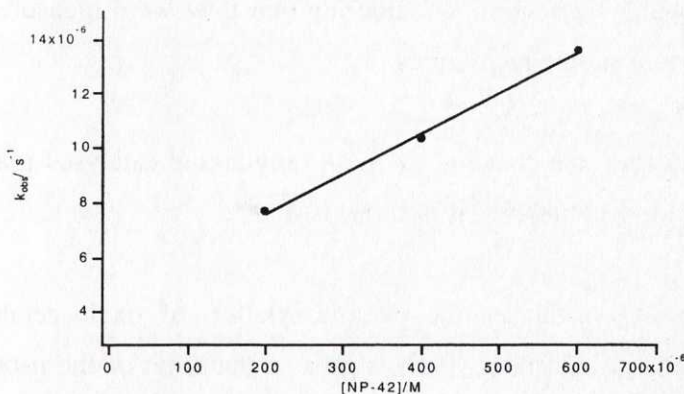


Figure 32. Plot of the pseudo first-order rate constant k_{obs} as a function of the peptide concentration. The calculated second-order rate constant for the peptide-catalysed reaction is $0.015 \text{ M}^{-1} \text{ s}^{-1}$.

7.4 The reactivity of NP-42

The measured second-order rate constants of the NP-42 catalysed reaction are presented in Table 1.

Table 1. The second-order rate constants for the decarboxylation of oxaloacetate.

catalyst	k_2 (or k_{cat}/K_M) / $\text{M}^{-1} \text{ s}^{-1}$
NP-42	0.01 ^a
NP-42	0.015 ^b
oxaldie 1	0.63 ^c
oxaldie 2	0.21 ^c
n-butylamine	0.0011 ^c

^a the rate constant obtained from the UV experiments. ^b the rate constant obtained from the NMR experiments. ^c reference 26.

The second-order rate constant calculated from the UV measurements is $0.01 \text{ M}^{-1} \text{ s}^{-1}$, and that from the NMR experiments is $0.015 \text{ M}^{-1} \text{ s}^{-1}$. They

are in reasonable agreement, considering that they were measured by two different spectroscopic techniques.

The second-order rate constant of the *n*-butylamine catalysed reaction has been reported, previously²⁶, it is $0.0011 \text{ M}^{-1} \text{ s}^{-1}$.

NP-42 therefore catalyses the decarboxylation of oxaloacetate with a second-order rate constant which is greater than that of the *n*-butylamine catalysed reaction by approximately a factor of ten. The reason for its enhanced reactivity has not yet been determined but it may be a combination of a depressed pK_a and transition state binding.

Attempts were also made to observe any reaction intermediate directly by ^1H NMR spectroscopy, but no such intermediate was detected.

The high catalytic efficiency of oxaldie 1 is to a great extent dependent upon the terminal amino group which has a low pK_a of approximately 7.2, due to interactions with the helix dipole. Binding by the cationic peptide of the anionic transition state is suggested as an additional reason for the high catalytic activity of the oxaldie peptide catalysts. Possible future enhancements of NP-42 reactivity might arise from moving the lysine residue within the reactive site, perhaps into the hydrophobic core in order to depress its pK_a and optimising the positions and number of the substrate binding arginine residues in the reactive site.

7.5 Summary

The NP-42 catalysed decarboxylation of oxaloacetate has been studied by both UV and ^1H NMR spectroscopy, where the latter allows direct measurement of changes of both the reactant and the product

concentration over time. The calculated second-order rate constants for the reaction as measured by UV and ^1H NMR spectroscopy were in reasonable agreement with each other and greater than that of the *n*-butylamine catalysed reaction by approximately a factor of 10.

8. Preparation of a cyclic hexapeptide model system for the study of transamination reactions

8.1 Cyclic hexapeptides

Cyclic hexapeptides can also be used as templates for enzyme mimicking model systems because the synthesis and purification of hexapeptides is relatively straightforward. They do, however, not have the large surface area of the folded polypeptides, and the introduction of complementary groups for binding and catalysis is more difficult. To explore the possibility of using a cyclic peptide as an enzyme model system, incorporation of a pyridoxal derivative as a bridge into a cyclic hexapeptide was attempted. It was expected to result in a transaminase mimic, designed to bind amino acids stereoselectively and to organise catalytic groups in a predetermined, reactive geometry.

8.2 Design of the cyclic hexapeptide

A pyridoxine derivative can be incorporated as a bridge that restricts the conformational freedom of a peptide. A schematic representation of the designed peptide is shown in Figure 33.

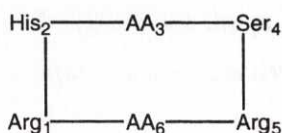


Figure 33. Schematic representation of the designed cyclohexapeptide. The incorporated pyridoxine derivative would link residues AA₃ and AA₆.

The amino acids AA-3 and AA-6 are the residues that are coupled to the bridging pyridoxine derivative. His-2 was introduced to function both as

the proton abstractor and as the proton donor in the transamination reaction, whereas Arg-1 was included to bind the carboxylate function of the substrate amino acid. Ser-4 and Arg-5 were incorporated to enhance the solubility in aqueous solutions.

8.3 Design and synthesis of a two-armed pyridoxine derivative for incorporation into a cyclohexapeptide

A two-armed pyridoxine derivative, shown in Figure 34, was designed for the

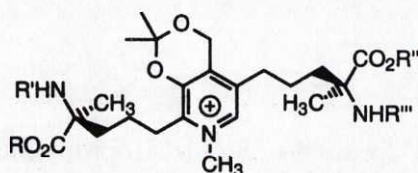
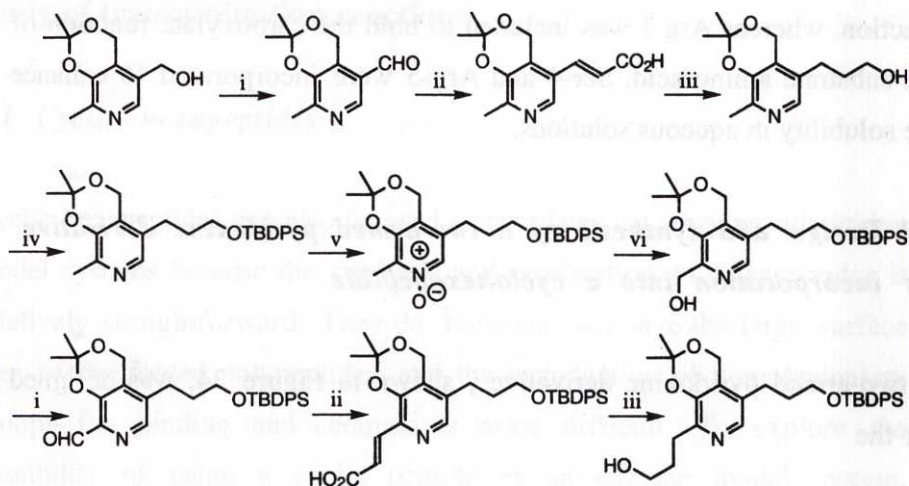


Figure 34. The designed two-armed pyridoxine derivative. R-R''' are different protecting groups

incorporation into the cyclic hexapeptide. The derivative was to be incorporated by sequential couplings of the amino acid moieties to the growing peptide chain, i.e. one arm was coupled while the other amino acid functionality remained protected. After the coupling of the intervening amino acids to the peptide chain, the second amino acid moiety would be deprotected and coupled to the peptide chain. The length of the two linkages in positions 2 and 5 of the pyridinium ring was chosen based on results from molecular modelling.

The synthetic strategy for the pyridoxine derivative was mainly based on methods published by Korytnyk⁴⁶, Scheme 2.

⁴⁶ a) Korytnyk, W. J. *Med. Chem.* 1965, 8, 112.



Scheme 2.

The synthesis started from the 3-*O*- α^4 -isopropylidene-pyridoxine⁴⁷ by oxidation to the corresponding aldehyde using MnO_2 , (i). The aldehyde was then transformed to the α,β -unsaturated acid through a Knoevenagel condensation with malonic acid, (ii). The unsaturated acid was reduced directly to the saturated alcohol with LiAlH_4 in THF, (iii). The alcohol was protected as a *t*-butyldiphenylsilyl ether through a DMAP-catalysed reaction⁴⁸, (iv). Oxidation of the silyl ether using MCPBA, (v), yielded the *N*-oxide, which was transformed to the 2'-alcohol in a TFAA-mediated rearrangement, (vi). The 2'-alcohol was then oxidised with MnO_2 , (i), the formed aldehyde was condensed with malonic acid, (ii), and the formed unsaturated acid was reduced as described for the 5-position, (iii).

The resulting alcohol was then to be transformed into a halide that can be used for the asymmetric alkylation of the α -carbon of an α -amino acid

b) Korytnyk, W.; Srivastava, S. C.; Angelino, N.; Potti, P. G. G.; Paul, B. *J. Med. Chem.* **1973**, 16, 1096.

⁴⁷ Wu, Y.-K.; Ahlberg, P. *Acta Chem. Scand.* **1989**, 43, 1009.

moiety, following which the other linkage could be deprotected and the free hydroxyl group treated in the same way as the former alcohol.

The TBDPS-protected alcohol was prepared in a low overall yield (ca. 2%).

8.4 Asymmetric α -amino acid synthesis

The pyridoxine derivative designed for incorporation into the cyclohexapeptide was to become a diamino acid derivative through asymmetric alkylation. There are a large number of methods of amino acid synthesis in the literature that give both good yields and products of high optical purity⁴⁹. Those most useful in our case were the methods of Mutter⁵⁰, Schöllkopf⁵¹, and Myers⁵².

8.4.1 The Mutter approach to α -methylated α -amino acids

This synthesis according to Mutter, Figure 35, is rather straightforward, with the

⁴⁸ Chaudhary, S. K.; Hernandez, O. *Tetrahedron Lett.* **1979**, 99.

⁴⁹ For two comprehensive reviews on asymmetric α -amino acid synthesis, see:

a) Williams, R. M. *Synthesis of optically active α -amino acids*, Vol. 7 of *Organic Chemistry Series*; Baldwin, J. E.; Magnus, P. D. (Eds); Pergamon Press, Oxford, **1989**.

b) Duthaler, R. O. *Tetrahedron* **1994**, *50*, 1539.

⁵⁰ Altmann, E.; Nebel, K.; Mutter, M. *Helvetica Chim. Acta* **1991**, *74*, 800.

⁵¹ a) Schöllkopf, U.; Hinrichs, R.; Lonsky, R. *Angew. Chem. Int. Ed. Engl.* **1987**, *26*, 143.

b) Schöllkopf, U.; Lonsky, R. *Synthesis* **1983**, 675.

⁵² a) Myers, A. G.; Bryant, H.; Yang, H. C.; Gleason, J. L. *J. Am. Chem. Soc.* **1994**, *116*, 9361.

b) Myers, A. G.; Gleason, J. L.; Yoon, T. *J. Am. Chem. Soc.* **1995**, *117*, 8488.

c) Myers, A. G.; Yoon, T.; Gleason, J. L. *Tetrahedron Lett.* **1995**, *36*, 4555.

d) Myers, A. G.; Gleason, J. L. *J. Org. Chem.* **1996**, *61*, 813.

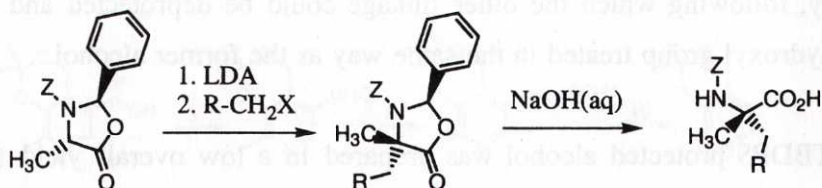


Figure 35. Mutter's oxazolidinone method of asymmetric α -amino acid synthesis. X=Br, I. Z=PhCH₂CO

only sensitive step being the enolisation of the oxazolidinone. The ring opening method shown in Figure 35 is the simplest of the alternatives, the other being that of catalytic hydrogenation. The oxazolidinone compound was prepared in modest yield, approximately 30 %. Attempts were made to utilise *N*-protecting groups other than Cbz, using Alloc-Cl and *t*-Boc-Cl. The *t*-Boc derivative was formed in small amounts, but could not be isolated. The Alloc derivative was not formed at all. The alkylation sequence failed to produce any significant amount of product. After several attempts, a 20 % yield of the *n*-pentyl alkylated oxazolidinone was isolated in model experiments.

8.4.2 The Schöllkopf bis-lactim ether method

The Schöllkopf *bis*-lactim ether method begins with the synthesis of an asymmetric *bis*-lactim ether using either alanine and valine, or glycine and valine, as starting amino acids. The *bis*-lactim ether is alkylated, through the sequence shown in Figure 36,

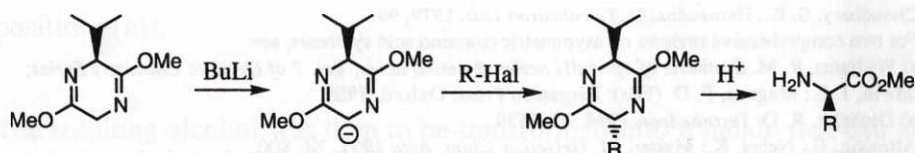


Figure 36. The *bis*-lactim ether method of Schöllkopf.

yielding a *trans* product. After the alkylation, the *bis*-lactim ether is hydrolysed under strongly acidic conditions to give an amino ester hydrochloride or an amino acid hydrochloride. Alkylation of the *bis*-lactim ether was performed as described in the literature and the yield was within the range reported. The work-up methods were not compatible with the protective groups required in the total synthesis of the di-amino acid derivative.

8.4.3 The pseudoephedrine method of Myers

The final method considered was the alkylation of the amino acid amides of pseudoephedrine, developed by Myers and co-workers. The reaction sequence of the method is given in Figure 37.

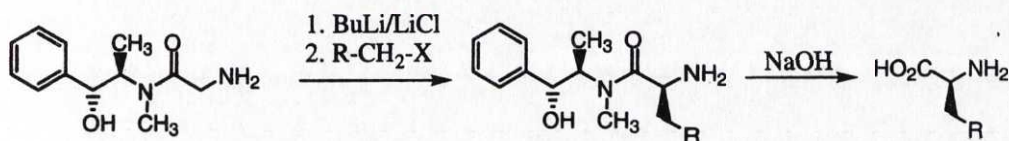


Figure 37. The pseudoephedrine method for asymmetric α -amino acid synthesis.

A variation of this method, using alanine instead of glycine, was also evaluated. The alkylations of the pseudoephedrine glycinamide proceeded according to the literature when simple alkyl halides were used, but when 1-bromo-3-phenylpropene was used as a model compound the yield decreased significantly. The alaninamide alkylations failed to produce any significant amount of product.

8.5 Summary

The amino acid syntheses showed that preparing a pyridoxine derivative, functionalised with an α -amino acid moiety at the end of each of two

Designed folded polypeptide model systems for the study of enzyme mimicking reactions

elongated side chains, would be time-consuming as well as difficult, although the synthesis of the pyridoxine derivative itself was performed. The project was abandoned in favour of the post-synthetic modification of polypeptides.



Figure 3. The pseudocatalytic method for enzymatic α -amino acid synthesis.

A variation of this method using amino instead of pyridoxine was also evaluated. The efficiency of the pseudocatalytic pyridoxine method according to the literature when using 20% inhibitor was also evaluated. 1-bromo-3-phenylpropane was used as a model substrate. The yield decreased significantly. The alkanamide alkylation failed to produce any



The amino acid synthesis showed that preparing a pyridoxine derivative functionalised with an α -amino acid moiety at the end of each of two

9. Summary and outlook

The design of model systems for the study of enzymatic reactions represents a considerable challenge. The knowledge gained, however, more than compensates for the labour involved because it can be applied in the engineering of new catalysts with novel functions and tailored specificities.

This thesis has shown that folded polypeptides can be used as templates in the design of model systems for enzyme mimicking reactions, and the first step in the engineering of three such catalysts have now been taken.

The incorporation of a NAD^+ model compound into LA-42 showed that the preparation of the polypeptide model system can be made in an efficient and straightforward manner and without affecting the structure of the polypeptide adversely.

The design of the reactive site in PP-42 went a step further in introducing non-covalent interactions as the controlling factor in the incorporation of the pyridoxal phosphate cofactor. The incorporation was shown to be site-selective and controlled by the interactions between the phosphate group of the cofactor and an arginine residue in the reactive site.

With NP-42 a first-generation folded polypeptide catalyst for the decarboxylation of oxaloacetate was designed and was shown to give rate enhancements over that of the *n*-butylamine catalysed reaction by approximately a factor of 10. NP-42 can now be used as a template for the reengineering of the reactive site towards greater catalytic efficiency in a rational manner.

Designed folded polypeptide model systems for the study of enzyme mimicking reactions

The cyclic hexapeptide model system was abandoned in favour of the folded polypeptides, mainly due to the time-consuming syntheses required. Also, the rigidity of such a system makes it necessary that the reactive site geometries are approximately correct in each attempt and the probability of success is therefore low.

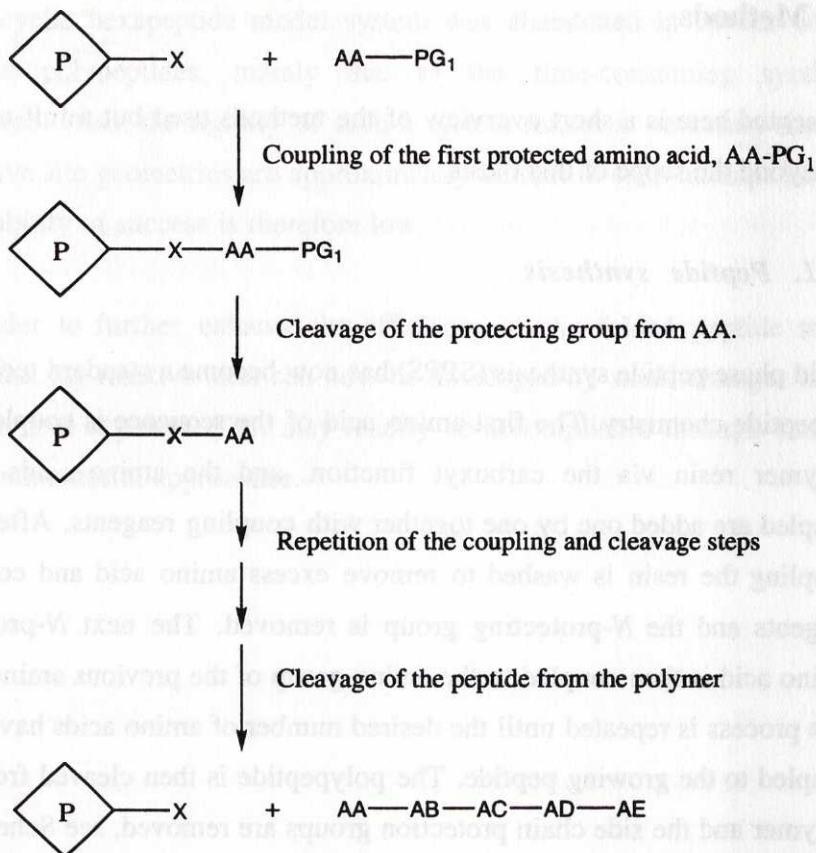
In order to further enhance the efficiency of the folded peptide model systems, the reactive sites can now be developed by small changes in the amino acid sequence. This may readily be accomplished through rational or combinatorial approaches.

10. Methods

Presented here is a short overview of the methods used but a full account is beyond the scope of this thesis.

10.1. Peptide synthesis

Solid phase peptide synthesis (SPPS) has now become a standard technique in peptide chemistry. The first amino acid of the sequence is coupled to a polymer resin via the carboxyl function, and the amino acids to be coupled are added one by one together with coupling reagents. After each coupling the resin is washed to remove excess amino acid and coupling reagents and the *N*-protecting group is removed. The next *N*-protected amino acid is then coupled to the amino group of the previous amino acid. The process is repeated until the desired number of amino acids have been coupled to the growing peptide. The polypeptide is then cleaved from the polymer and the side chain protection groups are removed, see Scheme 3.



Scheme 3.

In Scheme 3 has been presented an outline of the peptide synthesis, but the improvements and variations are many. Commonly used *N*-protection groups are *t*-Boc (*tert*-butyloxycarbonyl) and Fmoc (9-fluorenylmethyloxycarbonyl). The main difference between *t*-Boc and Fmoc chemistry is that *t*-Boc is removed by strong acid, usually TFA, and Fmoc is removed by base. The peptide-polymer linkage must therefore be stable towards strong acids in the case of *t*-Boc chemistry and the peptide has to be cleaved from the resin with the use of liquid HF, which leads to a number of impurities and side reactions. The Fmoc protection groups are removed with piperidine, which allows the use of a peptide-to-

polymer bond that is more easily cleaved than in the *t*-Boc strategy. In the Fmoc protocol the peptide is cleaved from the polymer by TFA, which is less damaging to the peptide.

In this investigation we have used a fully automated Fmoc SPPS protocol and a continuous-flow method.

10.2. HPLC

The mixture left after cleavage of the peptide from the polymer resin contains a lot of impurities like scavengers, remnants of protecting groups, cleavage reaction by-products, and deletion peptides and it is necessary to purify the peptide.

Synthesised peptides are readily purified by reverse-phase HPLC using isopropanol-water mixtures as eluent.

10.3. NMR spectroscopy

In structure determinations of polypeptides there are many powerful tools, but the most versatile is NMR spectroscopy. This technique can be used to study dynamics, dimer-monomer equilibria and three-dimensional structure.

Routine one-dimensional ^1H and ^{19}F NMR experiments, ^1H NMR NOESY (Nuclear Overhauser Spectroscopy), and TOCSY (Totally Correlated Spectroscopy) experiments have been used. In combination with ES-MS and CD spectroscopy they yield sufficient data for a three-dimensional structure to be determined. The NOESY experiment gives vital information about e.g. the structure of the hydrophobic core, whereas the

TOCSY spectrum gives information of the different amino acid residues and their chemical shifts.

10.4. CD spectroscopy

CD spectroscopy has been used only for comparisons of the mean residue ellipticities at 222 nm, Θ_{222} , of the synthesised or modified peptides and of RA-42.

10.5. Electrospray mass spectrometry

Electrospray mass spectrometry (ES-MS) is an excellent method for verifying the structure of a peptide. A solution containing the substance of interest is injected into the spectrometer through a capillary frit, where it is subjected to a high electric field, in the range of 10-20 kV. On the frit surface, charged micro droplets are formed and the solvent is removed by a counter current of inert gas. The ions, which now carry multiple charges, are accelerated in a magnetic field towards the mass analyser. The ions are then analysed, and their mass-to-charge ratio determined. The ES-MS spectrum shows series of peaks with the same m/z ratios, but carrying a different number of charges. These peaks are analysed after calibration and then transformed to give the molecular mass of the molecule.

11. Experimental

11.1 General

All glassware was washed thoroughly and oven-dried overnight at 150 °C or for 72 h at 55 °C. All air- and moisture-sensitive reactions were carried out in dry glassware under a positive pressure atmosphere of dry nitrogen gas. All air- and moisture-sensitive substances were transferred using gas-tight hypodermic syringes and septa. All solvents and reagents were dried and purified according to standard methods⁵³ when necessary, and otherwise used at commercial purity. Peptide synthesis was performed on a PerSeptive Biosystems Pioneer continuous-flow peptide synthesiser. All peptide synthesis chemicals and solvents were of the appropriate purity and were used at commercial purity. All buffer solutions were prepared from double-distilled water which was then filtered through a Millipore microfilter. All ¹H and ¹⁹F NMR spectra were recorded on a Varian Unity 500 FT-NMR spectrometer (9.395 T), except the two-dimensional experiments, which were performed on a Varian Unity 500 FT-NMR (11.744 T) spectrometer. Melting points were determined on a Reichert hot-stage microscope and are uncorrected. Optical rotations were measured on a Perkin-Elmer 241 polarimeter using the sodium D-line. HRMS was performed on a VG ZabSpec FD High resolution mass spectrometer. Flash chromatography (FC) was performed on silica gel S (230-400 mesh, 0.032-0.063 mm). Kinetic UV spectroscopy were performed on a Varian Cary 1 Bio UV-visible or a Varian Cary 4 spectrophotometer. CD spectra were recorded on a JASCO J-270 spectropolarimeter in the range from 300 to 190 nm. The instrument was calibrated with d-(+)-camphor sulphonic acid.

⁵³ Perrin, W. W.; Armarego, P. D. *Purification of Laboratory Chemicals*, 3rd ed. 1988, Pergamon Press.

11.2 Peptide synthesis and purification

Synthesis of NP-42

NP-42 was synthesised on Fmoc-Gly-PEG-PS resin (500 mg, 0.200 mmol/g substitution) with Fmoc-Gly attached. The entire synthesis was performed on a 0.100 millimolar scale. Fmoc chemistry was used throughout the entire synthesis. The peptide-containing resin was washed with DCM and dried *in vacuo*. The dry peptide was cleaved from the polymer with TFA (4.5 mL) using thioanisol (0.10 mL) and ethanedithiol (0.15 mL) as scavengers. The gel was then filtered, separating the peptide from the polymer, and washed with DCM. The free peptide was then precipitated with diethyl ether, centrifuged, and the supernatant ether removed. The crude peptide was then dissolved in water and lyophilised.

Synthesis of PP-42

PP-42 was synthesised in the same manner as NP-42.

Purification of NP-42

NP-42 was purified on a Varian Star HPLC system, using a preparative-scale C8 column. The solvent system used was 40 % isopropyl alcohol in a 0.1 % aqueous solution of TFA for the first run, and 38 % isopropyl alcohol in a 0.1 % aqueous solution of TFA for the second and final run. The collected fractions containing the peptide was lyophilised to yield the pure peptide.

ES-MS: 4515.729 (calc: 4516.09 gmol⁻¹)

Purification of PP-42

PP-42 was purified on a Varian Star HPLC system, using a preparative-scale C8 column. The solvent system used was 40 % isopropyl alcohol in a 0.1 % aqueous solution of TFA. The collected fractions containing the peptide was lyophilised to yield the pure peptide.

ES-MS: 4533.71 (calc: 4532.13 g mol^{-1})

11.3 Syntheses of the nonpeptide structures

11.3.1 NAD⁺ analogues and model systems

Nicotinic acid *p*-nitrophenyl ester (1)

This substance was prepared according to methods reported in the literature⁴². Nicotinic acid (0.522 g, 4.06 mmol), DCC (0.965 g, 4.68 mmol), and *p*-nitrophenol (0.650 g, 4.67 mmol) were dissolved in DCM (35 mL) and stirred at ambient temperature. 4-Pyrrolidinopyridine (63 mg, 0.4 mmol) in DCM (4 mL) was then added dropwise, causing the solution to turn yellow. The reaction mixture was stirred for six days at ambient temperature, after which it was washed with dilute HCl (aq, 1.1 M, 4 mL) and filtered to remove precipitated DCU. The filtrate was washed with HCl (30 mL, 0.4 M) and H₂O (50 mL), dried (Na₂SO₄), and the solvent removed at reduced pressure to yield the crude product. After recrystallisation from ethanol colourless needles were recovered in 92% yield (0.912 g).

Mp: 171 °C

¹H NMR (400 Mhz, CDCl₃) δ 9.41 (s, 1H), 8.91 (d, 1H), 8.47 (d, 2H), 8.36 (d, 2H), 7.51 (m, 1H), 7.45 (dd, 2H)

***N*-Methylnicotinic acid *p*-nitrophenyl ester iodide (2)**

This synthesis was prepared according to methods found in the literature⁵⁴. *p*-Nitrophenyl nicotinate (0.912 g, 3.74 mmol) was dissolved in DMF (5 mL), and methyl iodide (0.798 g, 5.62 mmol) was added. The reaction mixture was stirred in darkness for six days at ambient temperature. The solution turned red, probably due to oxidation of the iodide ion. The product was precipitated by the addition of diethyl ether (200 mL). The yield was almost quantitative.

¹H NMR (400 Mhz, DMSO) δ 9.81 (m, 1H), 9.26 (d, 1H) 9.18 (d, 1H), 8.44 (d, 2H), 8.35 (t, 1H), 7.71 (d, 2H), 4.41 (s, 3H)

FAB-MS: 259 gmol⁻¹ (calculated: 259.072)

***N*_ε-(*N*-methylnicotinoyl)-*L*-ornithine iodide (3)**

This substance was prepared using methods reported in the literature⁵⁵. *L*-Ornithine hydrochloride (0.40 g, 2.3 mmol) was dissolved in boiling water (50 mL). Copper carbonate (5.1 g) was then added, rendering the pH at approximately 6. Another portion of copper carbonate (1.2 g) was then added, raising the pH to ~7.5. The undissolved residues were filtered off from the now azure blue solution. A solution of NaHCO₃ (10 mL, 1.3 mmol) was then added, followed by *p*-nitrophenyl-*N*-methyl nicotinate (1.43 g, 3.7 mmol). After three min. a yellowish precipitation occurred, and the solution turned green. After 26 hours, the solution was acidified to pH 5 with HCl (1.2 M), causing CO₂(g) to be released. Diethyl ether extraction (4 x 60 mL) of *p*-nitrophenol gave yellow ethereal phases, and the aqueous phase regained its azure blue color. The aqueous solution was

⁵⁴ Murakami, Y.; Aoyama, Y.; Kikuchi, J.; Nishida, K. *J. Chem. Soc.*, **1982**, *104*, 5189.

⁵⁵ Sharp, J.; Goseny, I.; Rowley, A. *Practical Organic Chemistry*, 1st ed., Chapman and Hall, Cornwall, **1989**.

then subjected to $\text{H}_2\text{S}(\text{g})$ for 30 min., causing the solution to lose its colour while a brown-black precipitate of copper sulphide was formed. The precipitate was filtered off and water was removed from the filtrate under reduced pressure. Recrystallisation of the crude product from ethanol failed. Water was then added to the crude product, and after acidification the solution was stirred with ion exchange resin (2.04 g, Dowex 50W-X8 (H)). The mixture was left for 3-4 hours, after which the ion exchanger was packed in a column, and treated with ammonium hydroxide to release the product. Evaporation of the solvent in vacuo gave the product as a crystalline substance.

^1H NMR (400 MHz, D_2O) δ 9.1 (s, 1H), 8.8 (dd, 2H), 8.0 (t, 1H), 4.4 (s, 3H), 3.75 (m, 1H), 1.8 (m, 6H)

11.3.2 Syntheses of the cyclohexapeptide project

The nomenclature used in naming compounds 4-14 is based on the nomenclature used by Korytnyk⁴⁶.

3-O- α^4 -isopropylidene-pyridoxine (4)

This substance was prepared according to the literature⁴⁷.

3-O- α^4 -isopropylideneisopyridoxal (5)

This substance was prepared according to the literature⁵⁶.

3-O- α^4 -isopropylidene- α^5 -pyridoxylideneacetic acid (6)

This substance was prepared according to the literature⁴⁶.

⁵⁶ Brooks, Jr., H. G.; Laakso, J. W.; Metzler, D. E. *J. Heterocycl. Chem.* **1966**, *3*, 126.

3-*O*- α^4 -isopropylidene- α^5 -pyridoxylacetic acid (7)

This substance was prepared according to the literature⁴⁶.

2-(3-*O*- α^4 -isopropylidenepyridox-5-yl) ethanol (8)

This substance was prepared according to the literature⁴⁶.

2-(3-*O*- α^4 -Isopropylidenepyridox-5-yl) ethyl *t*-butyldiphenylsilyl ether (9)

This synthesis was based upon a general method reported in the literature⁴⁸. (The reason for using TBDPS instead of TBDMS was that TBDMS was not able to withstand the TFAA-mediated rearrangement below.) To a stirred solution of **8** (3.66 g, 15.4 mmol) in dry CH₂Cl₂ (150 mL) was added *t*-butyldiphenylsilyl chloride (4.00 mL, 1 eq.), triethylamine (1 eq), and a catalytic amount of DMAP. The reaction mixture was stirred under nitrogen at ambient temperature for 12-14 h. The solvent was then removed *in vacuo* and the residue taken up in ether. The ethereal solution was filtered twice to remove triethyl amine hydrochloride, washed once with water, and dried (Na₂SO₄). The solvent was evaporated to yield 7.25 g of the pure product as an oil. Yield: 99%.

¹H NMR (400 MHz, CDCl₃) δ 7.83 (s, 1H), 7.46 (d, 4H), 7.38 (m, 6H), 4.79 (s, 2H), 3.69 (t, 2H), 2.51 (t, 2H), 2.39 (s, 3H), 1.75 (t, 2H), 1.54 (s, 6H), 1.05 (s, 9H)

2-(3-*O*- α^4 -Isopropylidene-5-yl) ethyl *t*-butyldiphenylsilyl ether *N*-oxide (10)

This substance was prepared using a method from the literature⁴⁶. To a stirred solution of **9** (5.07 g, 10.6 mmol) in dry CHCl₃ (50 mL) was added dry MCPBA (1.1 eq) dissolved in CHCl₃ (25 mL) at 0 °C. The reaction mixture was then stirred at r.t. for 2 hours (until TLC indicated total consumption of reagents). The reaction mixture was then washed with NaHSO₃ (5%), NaHCO₃ (5%), and water. The solvent was removed *in vacuo*, and the crude oily product used without further purification in the next step.

¹H NMR (400 MHz, CDCl₃) δ 7.79 (s, 1H), 7.46 (d, 4H), 7.38 (m, 6H), 4.74 (s, 2H), 3.69 (t, 2H), 2.51 (t, 2H), 2.39 (s, 3H), 1.75 (t, 2H), 1.54 (s, 6H), 1.05 (s, 9H)

2-(3-*O*- α^4 -Isopropylidene-2'-hydroxy-norpyridox-5-yl) ethyl *t*-butyldiphenylsilyl ether (11)

This substance was prepared using a method from the literature⁴⁶. The crude *N*-oxide **10** from the former step was dissolved in CH₂Cl₂ (35 mL) and the solution cooled to 0 °C. To the stirred solution TFAA (1 mL) was then added by syringe. Another portion of TFAA (2.5 mL) was added 5 minutes later. The reaction mixture was allowed to warm to room temperature and then stirred at r.t. for 8-14 h. MeOH (15 mL) was added and the reaction mixture stirred for 30 min, and then washed with Na₂CO₃ (20%) and water. The solution was dried (Na₂SO₄) and the solvent evaporated to yield 3.71 g of crystalline **11**. Yield 90% over both steps.

When TBDMS was used as a protecting group, partial deprotection of the 5'-ethoxy group was evidenced in ¹H NMR, approximately 50-60% deprotection.

$^1\text{H NMR}$ (400 MHz, CDCl_3) δ 7.81 (s, 1H), 7.46 (d, 4H), 7.38 (m, 6H), 4.86 (s, 2H), 4.74 (s, 2H), 3.68 (t, 2H), 2.51 (t, 2H), 1.75 (t, 2H), 1.54 (s, 6H), 1.05 (s, 9H).

2-(3-*O*- α^4 -Isopropylidene-2-formyl-norpyridox-5-yl) ethyl *t*-butyldiphenylsilyl ether (12)

This substance was prepared using a method from the literature⁴⁶. The alcohol **11** (3.70 g, 9.0 mmol) was dissolved in CH_2Cl_2 (200 mL) and MnO_2 (act.~90%, ~7 eq, 15 g) was added. The heterogenous mixture was heated to reflux under nitrogen for 6 h (tlc monitoring). The reaction mixture was diluted with CH_2Cl_2 (50 mL) and treated with Celite. Celite and MnO_2 were removed by suction filtration. After evaporation of the solvent *in vacuo*, the crude aldehyde was used without further purification in the next step.

$^1\text{H NMR}$ (400 MHz, CDCl_3) δ 10.24 (s, 1H), 8.18 (s, 1H), 7.46 (d, 4H), 7.38 (m, 6H), 4.74 (s, 2H), 3.68 (t, 2H), 2.51 (t, 2H), 1.75 (t, 2H), 1.54 (s, 6H), 1.05 (s, 9H).

3-{3-*O*- α^4 -Isopropylidene-5-(3-[*t*-butyldiphenylsilyloxy]propyl)-2-pyridyl} propenoic acid (13)

This substance was prepared using the same method as for the preparation of **5**. The crude aldehyde **12** was dissolved in pyridine (25 mL), and piperidine (1 mL) and malonic acid (0.94 g, 9.0 mmol) was added. The reaction mixture was heated to 80 °C for 2 h and then stirred at r.t. overnight. Work-up was performed as with **5**. Yield 3.11 g, 64%.

$^1\text{H NMR}$ (400 MHz, CDCl_3) δ 7.98 (s, 1H), 7.95 (d, 1H), 7.46 (d, 4H), 7.38 (m, 6H), 6.95 (d, 1H), 4.74 (s, 2H), 3.68 (t, 2H), 2.51 (t, 2H), 1.75 (t, 2H), 1.54 (s, 6H), 1.05 (s, 9H).

2-(3-*O*- α^4 -Isopropylidene-2-(3'-hydroxypropyl)-norpyridox-5-yl) ethyl *t*-butyldiphenylsilyl ether (14)

This substance was prepared using a method from the literature⁴⁶. The acid **13** (1.0 g, 1.9 mmol) was dissolved in dry THF (120 mL) and the solution added dropwise to a suspension of LiAlH₄ (0.5 g) in dry THF (80 mL). The reaction mixture was stirred for 1h at r.t., following which the excess hydride was destroyed with ethyl acetate followed by water. After extracting the aqueous phase with ethyl acetate, the combined organic phases were dried (Na₂SO₄) and the solvent removed in vacuo, yielding the product as a yellow oil. Yield: 0.17 g (16%)

¹H NMR (400 MHz, CDCl₃) δ 7.98 (s, 1H), 7.46 (d, 4H), 7.38 (m, 6H), 4.74 (s, 2H), 3.68 (t, 2H), 3.05 (t, 3H), 2.71 (t, 2H), 2.51 (t, 2H), 1.65-1.75 (m, 4H), 1.54 (s, 6H), 1.05 (s, 9H).

(2*R*, 4*S*)-3-[benzyloxycarbonyl]-4-methyl-2-phenyl-1,3-oxazolidin-5-one (15)

This substance was prepared according to the literature⁵⁰.

Alkylation of 15

This reaction was performed according to the literature⁵⁰.

Alkylation of the *bis*-lactim ether of cyclo-L-Val-L-Ala (17)

This reaction was performed according to the literature⁵¹.

(*R,R*)-(-)-Pseudoephedrine glycineamide (18)

This substance was prepared according to the literature⁵².

(*R,R*)-(-)-Pseudoephedrine alanineamide (19)

This substance was prepared using methods reported in the literature⁵². *N*-*t*-Boc-Alanine (500 mg, 2.64 mmol) and Et₃N (442 μL, 1.2 eq.) was dissolved in dry DCM (10 mL) at 0 °C and trimethylacetyl chloride (0.39 mL, 2.64 mmol) was added dropwise under vigorous stirring. After 30 min. a second portion of Et₃N (442 μL, 1.2 eq.) and (*R,R*)-(-)-pseudoephedrine (437 mg, 2.64 mmol) were added sequentially. The reaction mixture was stirred for 45 minutes and the volatiles were removed *in vacuo*. The residue was taken up in a methanol-water mixture (10 mL, 1:1) and cooled in an ice bath. Conc. HCl (4 mL) was added, causing vigorous evolution of white fumes. After stirring for 3 h the methanol was removed *in vacuo* at 23 °C and the aqueous concentrate cooled in an ice bath while the pH was adjusted to 14, using 50 % NaOH. The aqueous solution was extracted with DCM (4 x 10 mL) and the combined extracts were dried (Na₂CO₃). The solution was filtered through Celite and the solvent removed to give white crystals that were recrystallised twice from toluene. The yield was 82.2 g.

Mp: 93.2-96.4 °C

¹H NMR (400 MHz, CDCl₃) δ 7.3–7.4 (m, 5H), 4.65 (d, 1H), 4.60 (d, 1H), 4.0-4.1 (m, 0.5H), 3.8 (d, 0.5H), 3.7 (d, 1H), 2.95 (s, 1.5H), 2.80 (s, 1.5H), 1.7 (s(broad), 3H), 1.4 (d, 1.5H), 1.09 (d, 1.5H), 1.05 (d, 1.5H), 0.98 (d, 1.5H).

Alkylation of (*R,R*)-(-)-Pseudoephedrine glycineamide (18)

This procedure was performed according to the literature⁵².

Alkylation of (*R,R*)-(-)-Pseudoephedrine alanineamide (19)

This procedure was performed according to methods reported in the literature⁵². The attempted alkylations of **19** were performed exactly as with **18**, but no product could be isolated.

11.4. Cofactor model incorporation

General procedure for cofactor model incorporation

The peptide (~4 mg) was dissolved in 400 μ L of Bis-Tris buffer at pH 5.9. The substrate was then added, and the mixture stirred on a shaking plate and left overnight. The salts in the mixture were removed by passing through a column of Sephadex GD-50 size-exclusion gel. The peptide was then lyophilised and purified by HPLC.

11.5 Kinetics and reaction studies

Background hydrolysis reaction of *N*-methylnicotinic acid *p*-nitrophenyl ester

Sodium acetate buffer (1.2 mL, 50 mM, pH 4.96) was transferred to an UV kuvette and tempered for 30 min. The NAD⁺ analogue (1.1 mg, ~2.8 μ mol) was dissolved in water (1.0 mL) and from this solution 80 μ L was added to the kuvette for a final concentration of 0.19 mM. The formation of *p*-nitrophenolate was monitored for several half-lives.

Kinetic measurement of NAD⁺ analogue incorporation into RA-42

RA-42 (1.2 mg, 27.4 μmol) was dissolved in sodium acetate (1.2 mL, 50 mM, pH 4.96) and the solution was placed in an UV kuvette and tempered for 30 min. Approximately 1/5 of a molar equivalent of the NAD⁺ analogue was added to the kuvette, and the formation of *p*-nitrophenolate was monitored for several half-lives. The product was purified and analysed by ES-MS, in order to determine the extent of incorporation.

Kinetic measurement of the reduction of 1-methylnicotinamide by sodium dithionite and sodium carbonate

1-Methylnicotinamide iodide (0.21 mg, 1.2 μmol) was dissolved in sodium phosphate buffer (400 μL , 50 mM, pH 7.02) to give a 3 mM solution, and the solution deoxygenated by passing nitrogen gas through it for several minutes. Sodium dithionite (1.04 mg, 5 eq.) and sodium carbonate (0.64 mg, 5 eq) was then added under nitrogen flow, following which the formation of the 1,4-dihydro-nicotinamide was monitored at 340 nm for several half-lives.

Incorporation of pyridoxal phosphate into PP-42

PP-42 (1.52 mg, 0.25 μmol based on 75% peptide content) was dissolved in Bis-Tris (500 μL , 50 mM) and 300 μL of the solution was transferred to a cuvette. PLP (in 50 mM Bis-Tris, 50 μL) was then added and the UV spectrum from 220 to 500 nm was studied at different concentrations of PLP and different pH.

Reduction of the aldimine between PP-42 and pyridoxal phosphate with NaBH₄

PP-42 (2.57 mg, 0.4 μ mol) was dissolved in a solution of PLP (5 mM, 400 μ L 50 mM Bis-Tris, pH 4.4) and the incorporation verified spectrophotometrically. The reaction mixture was then treated with NaBH₄ (100 μ L, 0.4 M in 10 mM NaOH), causing the reaction mixture to swiftly lose its yellow colour. A new absorbance at 290 nm appeared in the UV spectrum, while the aldimine absorbance at 389 disappeared. The mass of the reduced functionalized peptide was verified by LC-ESMS (4764.6).

Trypsin digestion of the reduced functionalised PP-42

The reduced functionalised PP-42 from the above experiment was treated with a solution of trypsin (1.4 mL of a solution of 2.02 mgs of trypsin in 100 mL 0.1 M NH₄CO₃ at pH 7.9) and the reaction mixture was kept at 37 °C for 3 h. The reaction mixture was acidified with HCl (60 μ L conc. HCl in 3 x 20 μ L portions), following which the mixture was lyophilized and analysed by LC-ESMS.

Transamination of L-glutamic acid by PP-42-bound pyridoxal phosphate

PP-42 (2.57 mg, 0.425 μ mol) was dissolved in a solution of PLP (0.3 mM, 400 μ L 50 mM Bis-Tris, pH 7.0) and the incorporation verified spectrophotometrically. The reaction mixture was then treated with a 26-fold excess of L-glutamic acid and the UV spectrum in the range of 220-500 nm monitored over time.

Decarboxylation of oxaloacetate using NP-42

Typical UV experiment

From a stock solution of NP-42 (0.23 mM in 50 mM BisTris at pH 7.0, I=0.15 (NaCl)) 300 μ L was transferred to a UV cuvette. Oxaloacetate (50 μ L, 70 mM in 50 mM Bis-Tris at pH 7.0, I=0.15, (NaCl)) was added and the absorbance at 285 nm followed for 360 min and the kinetic data processed using Igor Pro software.

Typical NMR experiment

From a stock solution of NP-42 (0.22 mM in 50 mM KH_2PO_4 at pH 7.0 (90% H_2O :10% D_2O)) 550 μ L was transferred to an NMR sample tube. Oxaloacetate (50 μ L, 120 mM in 50 mM KH_2PO_4 at pH 7.0 (90% H_2O :10% D_2O)) was added and the 1D ^1H NMR spectrum was recorded in an arrayed pre-acquisition delay experiment. The acquisition time was 0.992 s, the presaturation delay was 1.5 s, the number of scans per spectrum was 16 and the number of acquisitions was 60 with a delay of 60 seconds between each acquisition. The intensities of the oxaloacetate and puruvate resonances were then measured in each spectrum and the kinetic data processed using Igor Pro software.

12. Acknowledgements

First I would like to express my gratitude to my supervisor, Dr. Åke Nilsson, for his help, encouragement, and guidance during these years, and for introducing me to the discipline of organic chemistry.

I would also like to express my gratitude to the following people:

-Dr. Lars Baltzer, for help and guidance above and beyond the call of duty with peptide design, peptide and incorporation chemistry, NMR spectroscopy, constructive criticism of the manuscript and introducing me to the fields of modern NMR spectroscopy and polypeptide chemistry.

-Klas Broo, for successful teamwork, fruitful and interesting discussions, and being a true friend as well as a good room-mate. And also for all the fun we've had so far.

-Malin Allert for good and successful teamwork and also for last-minute pre-print help with the thesis.

-Professor Per Ahlberg for introducing me to the field of bioorganic chemistry.

-Linda Andersson, Pernilla Erlandsson, and Helena Nilsson for help with the peptide synthesiser, HPLC's, and odds and ends.

-Kerstin Broo and Annika Karlsson for good friendship over the years.

-Christian Appelt, Cecilia Farre, and Marie Sjöden for good teamwork on the amino acid and cofactor syntheses.

-Kerstin Bohman, Hans Svensson and Reine Torberntsson for their skilled help.

-Gunnar Stenhagen for help with the mass spectrometry.

-Charlotta Damberg of the Swedish NMR Centre for help with the spectrometers .

-Tommy Iliefski for good friendship and fun with the MacOS.

-All present and former members of the department for creating a good and friendly working atmosphere.

-Ulrika, for her neverending patience, love and support.

-My mother and father, for all their love and support.

-All my friends, for being what they are, real good friends.

-The boys and girls of a.n.t.U.

-JMS for doing B5.



Göteborg, May 4th, 1998.

På grund av upphovsrättsliga skäl kan vissa ingående delarbeten ej publiceras här.
För en fullständig lista av ingående delarbeten, se avhandlingens början.

Due to copyright law limitations, certain papers may not be published here.
For a complete list of papers, see the beginning of the dissertation.



GÖTEBORGS UNIVERSITET

6000138061



Göteborgs universitetsbibliotek

